National Aeronautics and
Space Administration

Lyndon B. Johnson Space Center

Recent Advancements in Fully Implicit Numerical Methods for Hypersonic Reacting Flows

with Application to Reentry and Arcjet Modeling

Benjamin S. Kirk[†], Roy H. Stogner[⋆],
Todd A. Oliver[⋆], and Paul T. Bauman[⋆]

[†] NASA Lyndon B. Johnson Space Center – Houston, TX USA
[⋆] Institute for Computational Engineering & Sciences – The University of Texas at Austin, USA

September 26, 2012

Acknowledgments

1. This work was supported in part by the Entry, Descent and Landing Project in the NASA/ESMD Enabling Technology Development and Demonstration Program.
2. This work was supported in part by a cooperative agreement with the Predictive Engineering and Computational Sciences (PECOS) Center at The University of Texas at Austin.
3. Thanks to Dr. Dinesh Prabhu (NASA/ARC) for providing the arcjet grids.

1. Background & Motivation
   - Problem Class
   - Reacting Flows
   - Surface Ablation
2. Physical Modeling
   - Governing Equations
   - Thermochemistry
   - Quasi-Steady Ablation
3. Finite Element Formulation
4. Fully-Implicit Navier-Stokes (FIN-S) Overview
   - Verification
   - Parallelism
5. Results
   - Perfect Gas Flow over a Double Cone
   - Viscous Thermal Equilibrium Chemical Reacting Flow
   - Viscous Reacting Flow with Quasi-Steady Surface Ablation
   - Modeling Arcjet Flows
6. Ongoing Challenges

1. Background & Motivation
   - Problem Class
   - Reacting Flows
   - Surface Ablation
2. Physical Modeling
   - Governing Equations
   - Thermochemistry
   - Quasi-Steady Ablation
3. Finite Element Formulation
4. Fully-Implicit Navier-Stokes (FIN-S) Overview
   - Verification
   - Parallelism
5. Results
   - Perfect Gas Flow over a Double Cone
   - Viscous Thermal Equilibrium Chemical Reacting Flow
   - Viscous Reacting Flow with Quasi-Steady Surface Ablation
   - Modeling Arcjet Flows
6. Ongoing Challenges

The physical phenomenon of interest is high-speed gas dynamics

Physics

- The compressible Navier-Stokes equations describe fluid flow for all Mach numbers.
- For aerospace applications of interest the Reynolds number is almost always such that the flows are *convection dominated*.
- *Multiscale phenomena* appear in the form of shock waves, boundary layers, and shear layers.

Numerics

- Discretization of the *conservation law form* of the Navier-Stokes equations is required for convergence to physically valid solutions.
- Convective terms must be treated with some form of *upwinding*.
- Shocks are treated with some form of *limiting* or *shock capturing*, both of which amount to artificial diffusion which regularizes the problem.

Aerodynamics

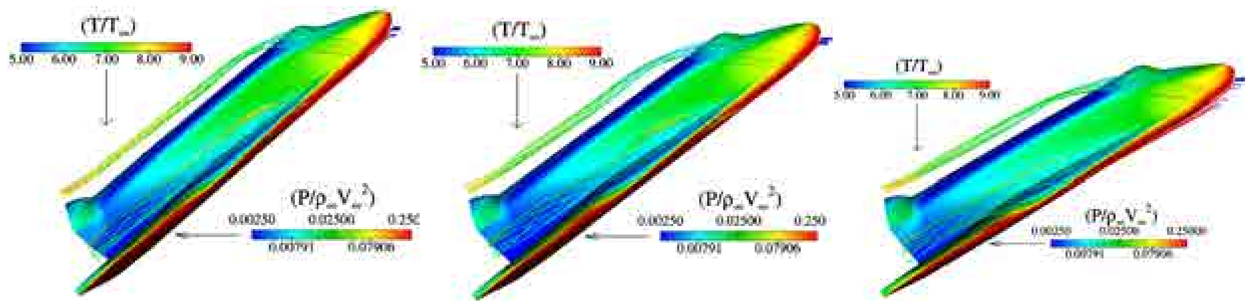

…is concerned with predicting aerodynamic forces and moments on a vehicle which result predominantly from the surface pressure distribution, but also from viscous shear stress.

Properly characterizing the aerodynamic performance of reentry vehicles is critical for optimal trajectory design.

Aerothermodynamics

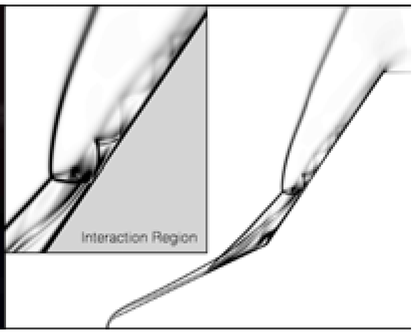

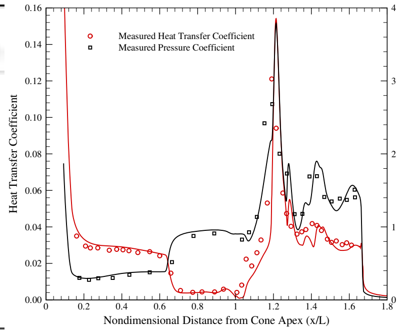

. . . is concerned with predicting the instantaneous total heat transfer rate and integrated heat load into a vehicle.

Properly characterizing this environment is crucial because it provides the design conditions for the thermal protection system:

heat transfer rate → thermal protection material selection
heat load → thermal protection material thickness

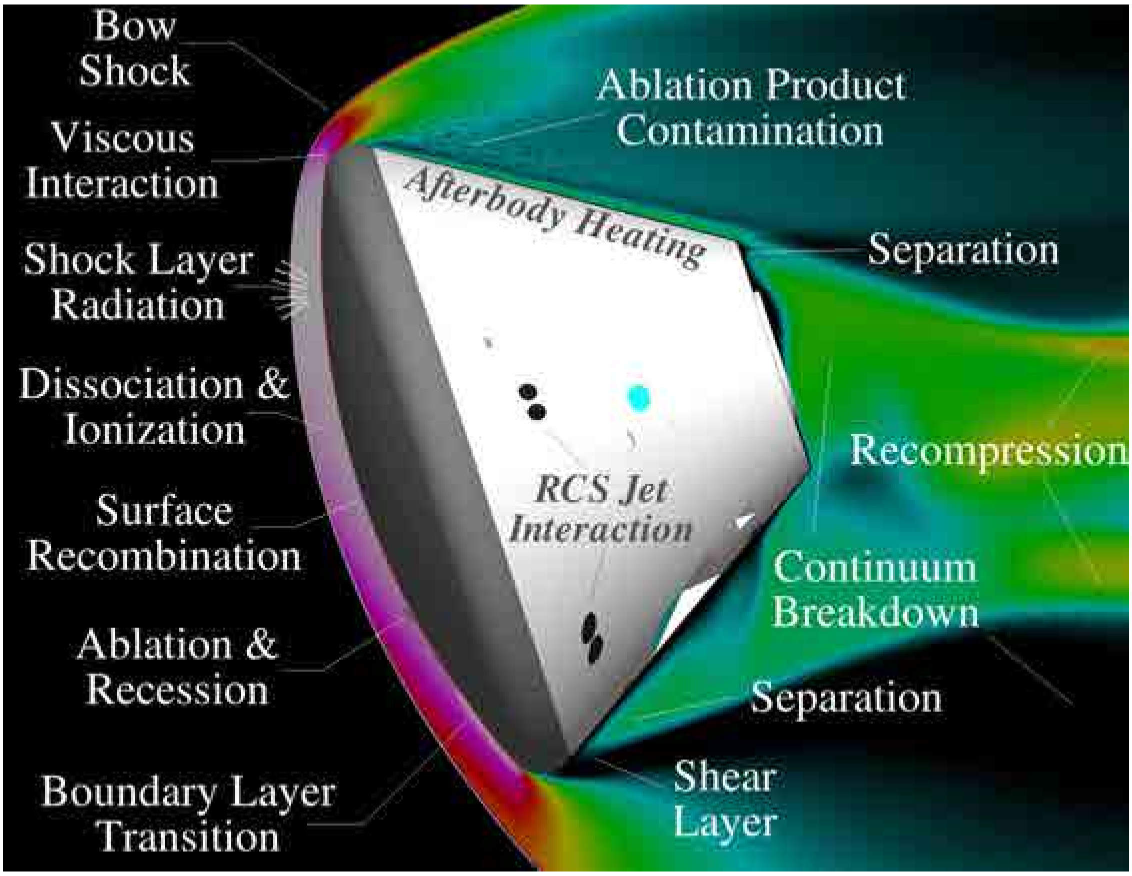

- When chemical kinetic timescales are approximately equal to flow timescales, the chemical composition of a flowfield must be determined as part of a simulation procedure. Such flows are in *chemical nonequilibrium*.

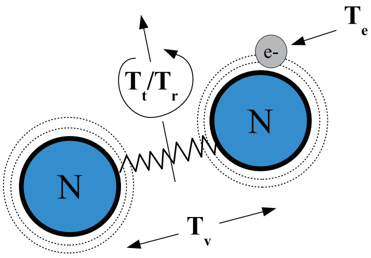

- Molecules and atoms can store energy in various *modes*.
- At hypersonic conditions these modes may not be in equilibrium, resulting in *thermal nonequilibrium*.

- The physical models and governing equations for flows in thermochemical nonequilibrium have been simulated previously with finite difference and finite volume techniques.
- In this work we review the physical models and implement a SUPG finite element scheme for hypersonic flows in thermochemical nonequilibrium.

- At hypersonic entry conditions, surface temperatures may exceed capabilities of reusable thermal protection system materials.
  - Reusable materials typically limited to $T < 2,000\,\mathrm{K}$.
  - It is necessary then to consider *ablative materials*.
- Ablative materials respond to high temperatures through pyrolysis, decomposition, blowing, and surface recession.
- Typically, ablation analysis is decoupled from the external flowfield, but we hope to do better.
- Additionally, accurately characterizing ground test facilities requires increased fidelity.

- As we will see, however, more accurate numerical modeling results in unique numerical challenges, necessitating novel numerical algorithms.

Governing Equations

- Extension from a single-species calorically perfect gas to a reacting mixture of thermally perfect gases requires species conservation equations and additional energy transport mechanisms.

$$\frac{\partial \rho_s}{\partial t} + \nabla \cdot (\rho_s \boldsymbol{u}) = \nabla \cdot (\rho \mathcal{D}_s \nabla c_s) + \dot{\omega}_s$$

$$\frac{\partial \rho \boldsymbol{u}}{\partial t} + \nabla \cdot (\rho \boldsymbol{u}\boldsymbol{u}) = -\nabla P + \nabla \cdot \boldsymbol{\tau}$$

$$\frac{\partial \rho E}{\partial t} + \nabla \cdot (\rho H \boldsymbol{u}) = -\nabla \cdot \dot{\boldsymbol{q}} + \nabla \cdot (\boldsymbol{\tau}\boldsymbol{u}) + \nabla \cdot \left(\rho \sum_{s=1}^{ns} h_s \mathcal{D}_s \nabla c_s \right)$$

- Problem class may also require a multitemperature thermal nonequilibrium option.

$$\frac{\partial \rho e_V}{\partial t} + \nabla \cdot (\rho e_V \boldsymbol{u}) = -\nabla \cdot \dot{\boldsymbol{q}}_V + \nabla \cdot \left(\rho \sum_{s=1}^{ns} e_{Vs} \mathcal{D}_s \nabla c_s \right) + \dot{\omega}_V$$

Turbulence Modeling

- We model the effects of turbulence using the Spalart-Allmaras one-equation turbulence model:

$$\frac{\partial}{\partial t}(\bar{\rho}\nu_{\mathrm{sa}}) + \frac{\partial}{\partial x_j}(\bar{\rho}\tilde{u}_j\nu_{\mathrm{sa}}) = c_{b1}S_{\mathrm{sa}}\bar{\rho}\nu_{\mathrm{sa}} - c_{w1}f_w\bar{\rho}\left(\frac{\nu_{\mathrm{sa}}}{d}\right)^2 + \frac{1}{\sigma}\frac{\partial}{\partial x_k}\left[(\mu+\bar{\rho}\nu_{\mathrm{sa}})\frac{\partial \nu_{\mathrm{sa}}}{\partial x_k}\right] + \frac{c_{b2}}{\sigma}\bar{\rho}\frac{\partial \nu_{\mathrm{sa}}}{\partial x_k}\frac{\partial \nu_{\mathrm{sa}}}{\partial x_k}$$

with closure terms

$$\mu_t = \bar{\rho}\nu_{\mathrm{sa}}f_{v1}, \qquad f_{v1} = \frac{\chi^3}{\chi^3 + c_{v1}^3}, \qquad f_{v2} = 1 - \frac{\chi}{1+\chi f_{v1}}, \qquad \chi = \frac{\nu_{\mathrm{sa}}}{\nu},$$

$$f_w = g\left(\frac{1+c_{w3}^6}{g^6 + c_{w3}^6}\right)^{1/6}, \qquad g = r + c_{w2}\left(r^6 - r\right), \qquad r = \frac{\nu_{\mathrm{sa}}}{S_{\mathrm{sa}}\kappa^2 d^2}.$$

Turbulence Modeling

- We model the effects of turbulence using the Spalart-Allmaras one-equation turbulence model:

$$\frac{\partial}{\partial t}(\bar{\rho}\nu_{\mathrm{sa}}) + \frac{\partial}{\partial x_j}(\bar{\rho}\tilde{u}_j\nu_{\mathrm{sa}}) = c_{b1}S_{\mathrm{sa}}\bar{\rho}\nu_{\mathrm{sa}} - c_{w1}f_w\bar{\rho}\left(\frac{\nu_{\mathrm{sa}}}{d}\right)^2 + \frac{1}{\sigma}\frac{\partial}{\partial x_k}\left[(\mu+\bar{\rho}\nu_{\mathrm{sa}})\frac{\partial \nu_{\mathrm{sa}}}{\partial x_k}\right] + \frac{c_{b2}}{\sigma}\bar{\rho}\frac{\partial \nu_{\mathrm{sa}}}{\partial x_k}\frac{\partial \nu_{\mathrm{sa}}}{\partial x_k}$$

and source term

$$S_{\mathrm{sa}} = \Omega + S_m, \quad S_{m0} = \frac{\nu_{\mathrm{sa}}}{\kappa^2 d^2}f_{v2}$$

where

$$S_m = \begin{cases} S_{m0}, & S_{m0} \geq -c_{v2}\Omega \\ \dfrac{\Omega(c_{v2}^2\Omega + c_{v3}S_{m0})}{((c_{v3}-2c_{v2})\Omega - S_{m0})}, & \text{otherwise.} \end{cases}$$

Thermodynamics & Transport Properties

- Thermochemistry models must be extended for a mixture of vibrationally and electronically excited thermally perfect gases.

$$\begin{aligned} e^{\text{int}} =& e^{\text{trans}} + e^{\text{rot}} + e^{\text{vib}} + e^{\text{elec}} + h^0 \\ =& \sum_{s=1}^{ns} c_s e_s^{\text{trans}}(T) + \sum_{s=mol} c_s e_s^{\text{rot}}(T) + \\ & \sum_{s=mol} c_s e_s^{\text{vib}}(T_V) + \sum_{s=1}^{ns} c_s e_s^{\text{elec}}(T_V) + \sum_{s=1}^{ns} c_s h_s^0 \end{aligned}$$

Here we have assumed that $T^{\text{trans}} = T^{\text{rot}} = T$ and $T^{\text{vib}} = T^{\text{elec}} = T_V$

- Additional transport property models are required. In this work we use
  - species viscosity given by Blottner curve fits,
  - species conductivities determined from an Eucken relation,
  - mixture transport properties computed via Wilke's mixing rule, and
  - mass diffusion currently treated by assuming constant Lewis number.

Chemical Kinetics & Energy Exchange

Kinetics:

- we consider r general reactions of the form

$$\begin{gathered} N_2 + \mathcal{M} \rightleftharpoons 2N + \mathcal{M} \\ \dots \\ N_2 + O \rightleftharpoons NO + N \\ \dots \end{gathered}$$

- When combined with forward and backward rates, these reactions produce the species source terms $\dot{\omega}_s$
- Presently, we use either CANTERA or an in-house library to provide these source terms.

Energy Exchange:

- Equilibration between the energy modes is modeled with a typical Landau-Teller vibrational energy exchange model with Millikan-White species relaxation times.
- Provides the vibrational energy source term $\dot{\omega}_V$

Chemical Kinetics

- We consider r general reactions of the form

$$N_2 + \mathcal{M} \rightleftharpoons 2N + \mathcal{M}$$
$$\dots$$
$$N_2 + O \rightleftharpoons NO + N$$
$$\dots$$

- The reactions are of the form

$$\mathcal{R}_r = k_{br} \prod_{s=1}^{ns} \left(\frac{\rho_s}{M_s} \right)^{\beta_{sr}} - k_{fr} \prod_{s=1}^{ns} \left(\frac{\rho_s}{M_s} \right)^{\alpha_{sr}}$$

where α_{sr} and β_{sr} are the stoichiometric coefficients for reactants and products

- The source terms are then

$$\dot{\omega}_s = M_s \sum_{r=1}^{nr} (\alpha_{sr} - \beta_{sr}) (\mathcal{R}_{br} - \mathcal{R}_{fr})$$

Energy Exchange

$$\dot{\omega}_V = \dot{Q}_v + \dot{Q}_{\text{transfer}}$$

We adopt the Landau-Teller vibrational energy exchange model

$$\dot{Q}_s^{\text{tr-vib}} = \rho_s \frac{\hat{e}_s^{\text{vib}} - e_s^{\text{vib}}}{\tau_s^{\text{vib}}}$$

where $\hat{e}_s^{\text{vib}}$ is the species equilibrium vibrational energy and the vibrational relaxation time τ_s^{vib} is given by Millikan and White

$$\tau_s^{\text{vib}} = \frac{\sum_{r=1}^{ns} \chi_r}{\sum_{r=1}^{ns} \chi_r / \tau_{sr}^{\text{vib}}}, \quad \chi_r = c_r \frac{M}{M_r}, \quad M = \left(\sum_{s=1}^{ns} \frac{c_s}{M_s} \right)^{-1}$$

and

$$\tau_{sr}^{\text{vib}} = \frac{1}{P} \exp \left[A_{sr} \left(T^{-1/3} - 0.015 \mu_{sr}^{1/4} \right) - 18.42 \right]$$
$$A_{sr} = 1.16 \times 10^{-3} \mu_{sr}^{1/2} \theta_{vs}^{4/3}, \quad \mu_{sr} = \frac{M_s M_r}{M_s + M_r}$$

Vibrational Energy Production and Energy Exchange

$$\dot{\omega}_V = \dot{Q}_v + \dot{Q}_{\text{transfer}}$$

When molecular species are created in the gas at rate $\dot{\omega}_s$, they contribute vibrational/electronic energy at the rate

$$\dot{Q}_{vs} = \dot{\omega}_s \left(e_s^{\text{vib}} + e_s^{\text{elec}} \right)$$

so the net vibrational energy production rate is

$$\dot{Q}_v = \sum_{s=1}^{ns} \dot{\omega}_s \left(e_s^{\text{vib}} + e_s^{\text{elec}} \right)$$

Combining terms yields the desired net vibrational energy source term

$$\dot{\omega}_V = \sum_{s=1}^{ns} \dot{Q}_s^{\text{tr-vib}} + \sum_{s=1}^{ns} \dot{\omega}_s \left(e_s^{\text{vib}} + e_s^{\text{elec}} \right)$$

Ablation Processes

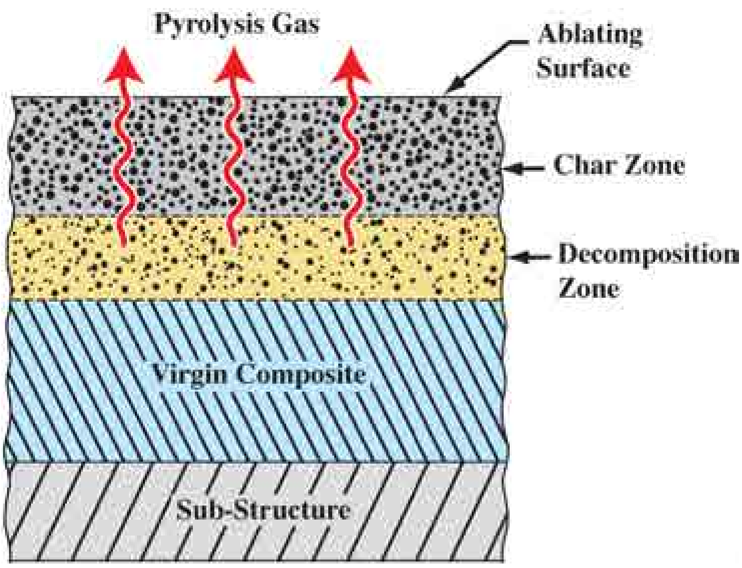

Schematic of ablation processes

- Ablation is a multi-scale, multi-physics phenomenon
- Sometimes amenable to simplification for predictive simulations

Quasi-steady State Ablation Hypothesis

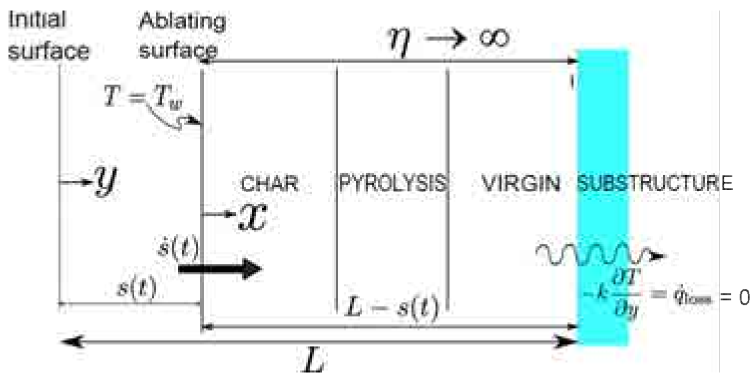

1. Steady state in reference frame fixed to the receding surface
2. Time variations solely due to motion of the material domain
3. Time scale for surface motion ($\dot{s} \approx 0.1 - 1$ mm/sec) much larger than characteristic time scale of unsteady processes
4. 1-D, semi-infinite medium

Quasi-steady Ablation

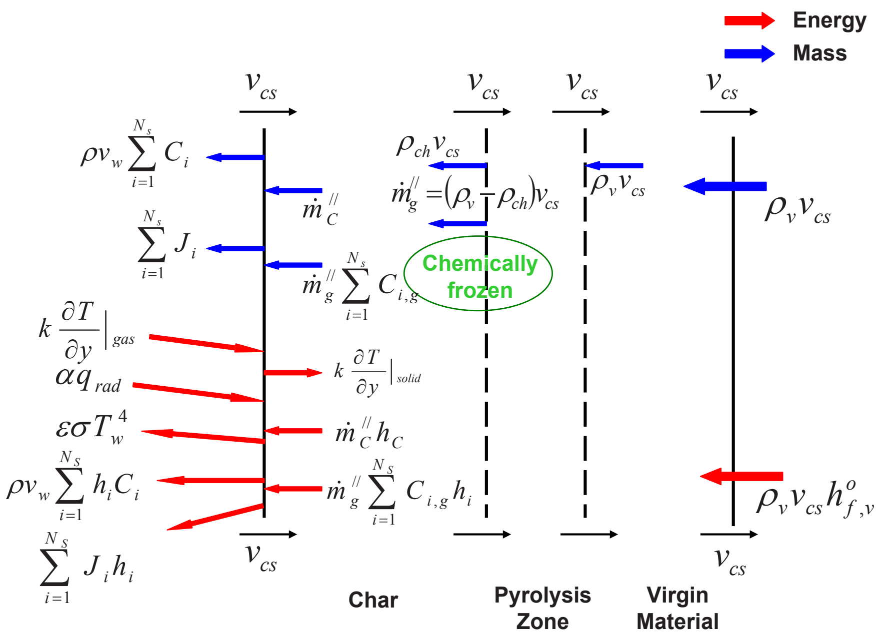

- Assumes ablation timescale $\ll$ trajectory timescale
- Assumes negligible substructure conduction

Ablation Interface Conditions

Recession:

$$\rho v_w = \dot{m}_c'' + \dot{m}_g''$$

Mass:

$$J_i|_{gas} + \rho v_w C_i = \tilde{N}_i(C_i, T) + \dot{m}_g'' C_{i,g}; (i : 1..N_s)$$

Energy:

$$- k\frac{\partial T}{\partial y}\bigg|_{gas} - \sum_{i=1}^{N_s} h_i(T_w)\, J_i|_{gas} + \dot{m}_c'' h_c(T) - \rho v_w h_w(T)$$

$$+\alpha \dot{q}_r'' - \sigma\epsilon {T_w}^4 + \sum_{i=1}^{N_s} \dot{m}_g'' C_{i,g} h_i(T_w) + k_s \frac{\partial T}{\partial y}|_{solid,w} = 0$$

- Nonlinear Robin Boundary Conditions
- Enables quasi-steady solves, restarts

Stabilized Finite Element Scheme

$$\frac{\partial \boldsymbol{U}}{\partial t} + \boldsymbol{A}_i \frac{\partial \boldsymbol{U}}{\partial x_i} = \frac{\partial}{\partial x_i}\left(\boldsymbol{K}_{ij}\frac{\partial \boldsymbol{U}}{\partial x_j}\right) + \dot{\boldsymbol{\mathcal{S}}}$$

Find $\boldsymbol{U}$ satisfying the essential boundary and initial conditions such that

$$\begin{aligned}
&\int_{\Omega}\left[\boldsymbol{W}\cdot\left(\frac{\partial \boldsymbol{U}}{\partial t} - \dot{\boldsymbol{\mathcal{S}}}\right) + \frac{\partial \boldsymbol{W}}{\partial x_i}\cdot\left(\boldsymbol{K}_{ij}\frac{\partial \boldsymbol{U}}{\partial x_j} - \boldsymbol{A}_i\boldsymbol{U}\right)\right] d\Omega \\
&+ \sum_{e=1}^{n_{el}}\int_{\Omega_e} \boldsymbol{\tau}_{\mathrm{SUPG}}\frac{\partial \boldsymbol{W}}{\partial x_k}\cdot\boldsymbol{A}_k\left[\frac{\partial \boldsymbol{U}}{\partial t} + \boldsymbol{A}_i\frac{\partial \boldsymbol{U}}{\partial x_i} - \frac{\partial \boldsymbol{G}_i}{\partial x_i} - \dot{\boldsymbol{\mathcal{S}}}\right] d\Omega \\
&+ \sum_{e=1}^{n_{el}}\int_{\Omega_e} \nu_{\mathrm{DCO}}\left(\frac{\partial \boldsymbol{W}}{\partial x_i}\cdot g^{ij}\frac{\partial \boldsymbol{U}}{\partial x_j}\right) d\Omega - \oint_{\Gamma}\boldsymbol{W}\cdot(\boldsymbol{g}-\boldsymbol{f})\ d\Gamma = 0
\end{aligned}$$

for all $\boldsymbol{W}$ in an appropriate function space.

Stabilization Parameters

Discontinuity capturing operator:

$$\nu_{\mathrm{DCO}} = \left[\frac{\left\|\frac{\partial \boldsymbol{U}}{\partial t} + \boldsymbol{A}_i\frac{\partial \boldsymbol{U}}{\partial x_i} - \frac{\partial}{\partial x_i}\left(\boldsymbol{K}_{ij}\frac{\partial \boldsymbol{U}}{\partial x_j}\right)\right\|^2_{\boldsymbol{A}_0^{-1}}}{(\Delta \boldsymbol{U}_h)^T\boldsymbol{A}_0^{-1}\Delta\boldsymbol{U}_h + g^{ij}\left(\frac{\partial \boldsymbol{U}_h}{\partial x_i}\right)^T\boldsymbol{A}_0^{-1}\frac{\partial \boldsymbol{U}_h}{\partial x_j}}\right]^{1/2}$$

SUPG stabilization matrix:

$$\boldsymbol{\tau}_{\mathrm{SUPG}}^{-1} = \sum_{i=\mathrm{nodes}}\left(\left|\frac{\partial \phi_i}{\partial x_j}\boldsymbol{A}_j\right| + \frac{\partial \phi_i}{\partial x_j}\boldsymbol{K}_{jk}\frac{\partial \phi_i}{\partial x_k}\right)$$

where

$$\left|\frac{\partial \phi_i}{\partial x_j}\boldsymbol{A}_j\right| = \boldsymbol{L}\,|\boldsymbol{\Lambda}|\,\boldsymbol{R}$$

Fully-Implicit Navier-Stokes (FIN-S)

Implementation Highlights

- C++ application code built on top of the `libMesh` library.
  - `libMesh` provides all requisite finite element data, parallel domain decomposition details.
  - Inherits PETSc preconditioned Krylov iterative solvers.
  - CANTERA used for kinetic rates, in-house thermodynamics, transport properties.
  - Only $\approx$ 30K SLOC
- Fully-coupled (monolithic solves), fully-implicit discretization.
- Rigorous verification using MASA-provided manufactured solutions.
- Testbed for intrusive VV/UQ schemes applied to hypersonics.

Manufactured Analytical Solution Abstraction Library

- Dearth of exact solutions necessitates *method of manufactured solutions*
- Some manufactured solutions exist for the calorically perfect Navier-Stokes equations
  - Developed in large part by Sandia National Labs
  - Specific solutions for field, boundary condition order-of-accuracy verification
- Existing solutions provide a necessary but not sufficient test suite
  - Will need to develop many more solutions to verify reacting flows with complex transport models
- Manufactured solutions are a valuable resource that should be accessible to anyone
- PECOS is developing the Manufactured Analytical Solution Abstraction (MASA) library to provide well-defined manufactured solutions and source terms for a range of physics applications

Manufactured solutions are being constructed and will be incorporated into the FIN-S regression test suite

Manufactured analytical solutions (used by Roy, Smith, and Ober) for each one of the primitive variables in Navier-Stokes equations are:

$$\rho\left(x,y\right) = \rho_0 + \rho_x \sin\left(\frac{a_{\rho x}\pi x}{L}\right) + \rho_y \cos\left(\frac{a_{\rho y}\pi y}{L}\right),$$
$$u\left(x,y\right) = u_0 + u_x \sin\left(\frac{a_{ux}\pi x}{L}\right) + u_y \cos\left(\frac{a_{uy}\pi y}{L}\right),$$
$$v\left(x,y\right) = v_0 + v_x \cos\left(\frac{a_{vx}\pi x}{L}\right) + v_y \sin\left(\frac{a_{vy}\pi y}{L}\right),$$
$$p\left(x,y\right) = p_0 + p_x \cos\left(\frac{a_{px}\pi x}{L}\right) + p_y \sin\left(\frac{a_{py}\pi y}{L}\right)$$

The method of manufactured solutions applied to Navier-Stokes equations requires modifying the governing equations by adding a source term to the right-hand side of each equation:

$$
\begin{aligned}
&\frac{\partial \rho}{\partial t} + \frac{\partial \rho u}{\partial x} + \frac{\partial \rho v}{\partial y} = Q_\rho \\
&\frac{\partial \rho u}{\partial t} + \frac{\partial \rho u^2 + p - \tau_{xx}}{\partial x} + \frac{\partial \rho u v - \tau_{xy}}{\partial y} = Q_u \\
&\frac{\partial \rho v}{\partial t} + \frac{\partial \rho v u - \tau_{yx}}{\partial x} + \frac{\partial \rho v^2 + p - \tau_{yy}}{\partial y} = Q_v \\
&\frac{\partial \rho e_t}{\partial t} + \frac{\partial \rho u e_t + p u - u\tau_{xx} - v\tau_{xy} + q_x}{\partial x} + \frac{\partial \rho v e_t + p v - u\tau_{yx} - v\tau_{yy} + q_y}{\partial y} = Q_{e_t}
\end{aligned}
$$

so the modified set of equations has a known, analytical solution. Symbolic representations of requisite source terms and C-source code have recently been generated for 2D and 3D calorically perfect gas flows.

$$
\begin{aligned}
Q_\rho = {} & \frac{a_{\rho x}\pi\rho_x}{L}\cos\left(\frac{a_{\rho x}\pi x}{L}\right)\left[u_x \sin\left(\frac{a_{ux}\pi x}{L}\right) + u_y \cos\left(\frac{a_{uy}\pi y}{L}\right) + u_0\right] \\
& - \frac{a_{\rho y}\pi\rho_y}{L}\sin\left(\frac{a_{\rho y}\pi y}{L}\right)\left[v_x \cos\left(\frac{a_{vx}\pi x}{L}\right) + v_y \sin\left(\frac{a_{vy}\pi y}{L}\right) + v_0\right] \\
& + \frac{a_{ux}\pi u_x}{L}\cos\left(\frac{a_{ux}\pi x}{L}\right)\left[\rho_x \sin\left(\frac{a_{\rho x}\pi x}{L}\right) + \rho_y \cos\left(\frac{a_{\rho y}\pi y}{L}\right) + \rho_0\right] \\
& + \frac{a_{vy}\pi v_y}{L}\cos\left(\frac{a_{vy}\pi y}{L}\right)\left[\rho_x \sin\left(\frac{a_{\rho x}\pi x}{L}\right) + \rho_y \cos\left(\frac{a_{\rho y}\pi y}{L}\right) + \rho_0\right]
\end{aligned}
$$

$$
\begin{aligned}
Q_u - {} & \frac{a_{px}\pi p_x}{L}\sin\left(\frac{a_{px}\pi x}{L}\right) \\
& + \frac{a_{\rho x}\pi\rho_x}{L}\cos\left(\frac{a_{\rho x}\pi x}{L}\right)\left[u_x \sin\left(\frac{a_{ux}\pi x}{L}\right) + u_y \cos\left(\frac{a_{uy}\pi y}{L}\right) + u_0\right]^2 \\
& - \frac{a_{\rho y}\pi\rho_y}{L}\sin\left(\frac{a_{\rho y}\pi y}{L}\right)\left[v_x \cos\left(\frac{a_{vx}\pi x}{L}\right) + v_y \sin\left(\frac{a_{vy}\pi y}{L}\right) + v_0\right]\left[u_x \sin\left(\frac{a_{ux}\pi x}{L}\right) + u_y \cos\left(\frac{a_{uy}\pi y}{L}\right) + u_0\right] \\
& + \frac{2a_{ux}\pi u_x}{L}\cos\left(\frac{a_{ux}\pi x}{L}\right)\left[u_x \sin\left(\frac{a_{ux}\pi x}{L}\right) + u_y \cos\left(\frac{a_{uy}\pi y}{L}\right) + u_0\right]\left[\rho_x \sin\left(\frac{a_{\rho x}\pi x}{L}\right) + \rho_y \cos\left(\frac{a_{\rho y}\pi y}{L}\right) + \rho_0\right] \\
& - \frac{\pi a_{uy} u_y}{L}\sin\left(\frac{a_{uy}\pi y}{L}\right)\left[v_x \cos\left(\frac{a_{vx}\pi x}{L}\right) + v_y \sin\left(\frac{a_{vy}\pi y}{L}\right) + v_0\right]\left[\rho_x \sin\left(\frac{a_{\rho x}\pi x}{L}\right) + \rho_y \cos\left(\frac{a_{\rho y}\pi y}{L}\right) + \rho_0\right] \\
& + \frac{\pi a_{vy} v_y}{L}\cos\left(\frac{a_{vy}\pi y}{L}\right)\left[u_x \sin\left(\frac{a_{ux}\pi x}{L}\right) + u_y \cos\left(\frac{a_{uy}\pi y}{L}\right) + u_0\right]\left[\rho_x \sin\left(\frac{a_{\rho x}\pi x}{L}\right) + \rho_y \cos\left(\frac{a_{\rho y}\pi y}{L}\right) + \rho_0\right] \\
& + \frac{4a_{ux}^2\pi^2\mu u_x}{3L^2}\sin\left(\frac{a_{ux}\pi x}{L}\right) + \frac{a_{uy}^2\pi^2\mu u_y}{L^2}\cos\left(\frac{a_{uy}\pi y}{L}\right)
\end{aligned}
$$

$$
\begin{aligned}
Q_v = {} & \frac{a_{py}\pi p_y}{L}\cos\left(\frac{a_{py}\pi y}{L}\right) \\
& + \frac{\pi a_{\rho x}\rho_x}{L}\cos\left(\frac{a_{\rho x}\pi x}{L}\right)\left[v_x \cos\left(\frac{a_{vx}\pi x}{L}\right) + v_y \sin\left(\frac{a_{vy}\pi y}{L}\right) + v_0\right]\left[u_x \sin\left(\frac{a_{ux}\pi x}{L}\right) + u_y \cos\left(\frac{a_{uy}\pi y}{L}\right) + u_0\right] \\
& - \frac{a_{\rho y}\pi\rho_y}{L}\sin\left(\frac{a_{\rho y}\pi y}{L}\right)\left[v_x \cos\left(\frac{a_{vx}\pi x}{L}\right) + v_y \sin\left(\frac{a_{vy}\pi y}{L}\right) + v_0\right]^2 \\
& + \frac{a_{ux}\pi u_x}{L}\cos\left(\frac{a_{ux}\pi x}{L}\right)\left[v_x \cos\left(\frac{a_{vx}\pi x}{L}\right) + v_y \sin\left(\frac{a_{vy}\pi y}{L}\right) + v_0\right]\left[\rho_x \sin\left(\frac{a_{\rho x}\pi x}{L}\right) + \rho_y \cos\left(\frac{a_{\rho y}\pi y}{L}\right) + \rho_0\right] \\
& - \frac{a_{vx}\pi v_x}{L}\sin\left(\frac{a_{vx}\pi x}{L}\right)\left[u_x \sin\left(\frac{a_{ux}\pi x}{L}\right) + u_y \cos\left(\frac{a_{uy}\pi y}{L}\right) + u_0\right]\left[\rho_x \sin\left(\frac{a_{\rho x}\pi x}{L}\right) + \rho_y \cos\left(\frac{a_{\rho y}\pi y}{L}\right) + \rho_0\right] \\
& + \frac{2a_{vy}\pi v_y}{L}\cos\left(\frac{a_{vy}\pi y}{L}\right)\left[v_x \cos\left(\frac{a_{vx}\pi x}{L}\right) + v_y \sin\left(\frac{a_{vy}\pi y}{L}\right) + v_0\right]\left[\rho_x \sin\left(\frac{a_{\rho x}\pi x}{L}\right) + \rho_y \cos\left(\frac{a_{\rho y}\pi y}{L}\right) + \rho_0\right] \\
& + \frac{a_{vx}^2\pi^2\mu v_x}{L^2}\cos\left(\frac{a_{vx}\pi x}{L}\right) + \frac{4a_{vy}^2\pi^2\mu v_y}{3L^2}\sin\left(\frac{a_{vy}\pi y}{L}\right)
\end{aligned}
$$

$$
\begin{aligned}
Q_{e_t} = {} & -\frac{a_{px}\pi p_x}{L}\frac{\gamma}{\gamma-1}\sin\left(\frac{a_{px}\pi x}{L}\right)\left[u_x \sin\left(\frac{a_{ux}\pi x}{L}\right) + u_y \cos\left(\frac{a_{uy}\pi y}{L}\right) + u_0\right] \\
& + \frac{a_{py}\pi p_y}{L}\frac{\gamma}{\gamma-1}\cos\left(\frac{a_{py}\pi y}{L}\right)\left[v_x \cos\left(\frac{a_{vx}\pi x}{L}\right) + v_y \sin\left(\frac{a_{vy}\pi y}{L}\right) + v_0\right] \\
& + \frac{a_{\rho x}\pi\rho_x}{2L}\cos\left(\frac{a_{\rho x}\pi x}{L}\right)\left[u_x \sin\left(\frac{a_{ux}\pi x}{L}\right) + u_y \cos\left(\frac{a_{uy}\pi y}{L}\right) + u_0\right]\left[\left[u_x \sin\left(\frac{a_{ux}\pi x}{L}\right) + u_y \cos\left(\frac{a_{uy}\pi y}{L}\right) + u_0\right]^2 + \left[v_x \cos\left(\frac{a_{vx}\pi x}{L}\right) + v_y \sin\left(\frac{a_{vy}\pi y}{L}\right) + v_0\right]^2\right] \\
& - \frac{a_{\rho y}\pi\rho_y}{2L}\sin\left(\frac{a_{\rho y}\pi y}{L}\right)\left[v_x \cos\left(\frac{a_{vx}\pi x}{L}\right) + v_y \sin\left(\frac{a_{vy}\pi y}{L}\right) + v_0\right]\left[\left[u_x \sin\left(\frac{a_{ux}\pi x}{L}\right) + u_y \cos\left(\frac{a_{uy}\pi y}{L}\right) + u_0\right]^2 + \left[v_x \cos\left(\frac{a_{vx}\pi x}{L}\right) + v_y \sin\left(\frac{a_{vy}\pi y}{L}\right) + v_0\right]^2\right] \\
& + \frac{a_{ux}\pi u_x}{2L}\cos\left(\frac{a_{ux}\pi x}{L}\right)\left\{\left[p_x \cos\left(\frac{a_{px}\pi x}{L}\right) + p_y \sin\left(\frac{a_{py}\pi y}{L}\right) + p_0\right]\frac{2\gamma}{\gamma-1} + \right. \\
& \qquad \left. + \left[3\left[u_x \sin\left(\frac{a_{ux}\pi x}{L}\right) + u_y \cos\left(\frac{a_{uy}\pi y}{L}\right) + u_0\right]^2 + \left[v_x \cos\left(\frac{a_{vx}\pi x}{L}\right) + v_y \sin\left(\frac{a_{vy}\pi y}{L}\right) + v_0\right]^2\right]\left[\rho_x \sin\left(\frac{a_{\rho x}\pi x}{L}\right) + \rho_y \cos\left(\frac{a_{\rho y}\pi y}{L}\right) + \rho_0\right]\right\} \\
& - \frac{a_{uy}\pi u_y}{L}\sin\left(\frac{a_{uy}\pi y}{L}\right)\left[\rho_x \sin\left(\frac{a_{\rho x}\pi x}{L}\right) + \rho_y \cos\left(\frac{a_{\rho y}\pi y}{L}\right) + \rho_0\right]\left[u_x \sin\left(\frac{a_{ux}\pi x}{L}\right) + u_y \cos\left(\frac{a_{uy}\pi y}{L}\right) + u_0\right]\left[v_x \cos\left(\frac{a_{vx}\pi x}{L}\right) + v_y \sin\left(\frac{a_{vy}\pi y}{L}\right) + v_0\right] \\
& - \frac{a_{vx}\pi v_x}{L}\sin\left(\frac{a_{vx}\pi x}{L}\right)\left[\rho_x \sin\left(\frac{a_{\rho x}\pi x}{L}\right) + \rho_y \cos\left(\frac{a_{\rho y}\pi y}{L}\right) + \rho_0\right]\left[u_x \sin\left(\frac{a_{ux}\pi x}{L}\right) + u_y \cos\left(\frac{a_{uy}\pi y}{L}\right) + u_0\right]\left[v_x \cos\left(\frac{a_{vx}\pi x}{L}\right) + v_y \sin\left(\frac{a_{vy}\pi y}{L}\right) + v_0\right] \\
& + \frac{a_{vy}\pi v_y}{2L}\cos\left(\frac{a_{vy}\pi y}{L}\right)\left\{\left[p_x \cos\left(\frac{a_{px}\pi x}{L}\right) + p_y \sin\left(\frac{a_{py}\pi y}{L}\right) + p_0\right]\frac{2\gamma}{\gamma-1}\right. \\
& \qquad \left. + \left[\left[u_x \sin\left(\frac{a_{ux}\pi x}{L}\right) + u_y \cos\left(\frac{a_{uy}\pi y}{L}\right) + u_0\right]^2 + 3\left[v_x \cos\left(\frac{a_{vx}\pi x}{L}\right) + v_y \sin\left(\frac{a_{vy}\pi y}{L}\right) + v_0\right]^2\right]\left[\rho_x \sin\left(\frac{a_{\rho x}\pi x}{L}\right) + \rho_y \cos\left(\frac{a_{\rho y}\pi y}{L}\right) + \rho_0\right]\right\} \\
& + \frac{a_{px}^2\pi^2 k\, p_x \cos\left(\frac{a_{px}\pi x}{L}\right)}{\left[\rho_x \sin\left(\frac{a_{\rho x}\pi x}{L}\right) + \rho_y \cos\left(\frac{a_{\rho y}\pi y}{L}\right) + \rho_0\right] L^2 R} + \frac{a_{py}^2\pi^2 k\, p_y \sin\left(\frac{a_{py}\pi y}{L}\right)}{\left[\rho_x \sin\left(\frac{a_{\rho x}\pi x}{L}\right) + \rho_y \cos\left(\frac{a_{\rho y}\pi y}{L}\right) + \rho_0\right] L^2 R} \\
& - \frac{2a_{\rho x}^2\pi^2 k\,\rho_x^2}{L^2 R}\cos^2\left(\frac{a_{\rho x}\pi x}{L}\right)\frac{\left[p_x \cos\left(\frac{a_{px}\pi x}{L}\right) + p_y \sin\left(\frac{a_{py}\pi y}{L}\right) + p_0\right]}{\left[\rho_x \sin\left(\frac{a_{\rho x}\pi x}{L}\right) + \rho_y \cos\left(\frac{a_{\rho y}\pi y}{L}\right) + \rho_0\right]^3} - \frac{a_{\rho x}^2\pi^2 k\rho_x}{L^2 R}\sin\left(\frac{a_{\rho x}\pi x}{L}\right)\frac{\left[p_x \cos\left(\frac{a_{px}\pi x}{L}\right) + p_y \sin\left(\frac{a_{py}\pi y}{L}\right) + p_0\right]}{\left[\rho_x \sin\left(\frac{a_{\rho x}\pi x}{L}\right) + \rho_y \cos\left(\frac{a_{\rho y}\pi y}{L}\right) + \rho_0\right]^2} \\
& - \frac{2a_{\rho y}^2\pi^2 k\,\rho_y^2}{L^2 R}\sin^2\left(\frac{a_{\rho y}\pi y}{L}\right)\frac{\left[p_x \cos\left(\frac{a_{px}\pi x}{L}\right) + p_y \sin\left(\frac{a_{py}\pi y}{L}\right) + p_0\right]}{\left[\rho_x \sin\left(\frac{a_{\rho x}\pi x}{L}\right) + \rho_y \cos\left(\frac{a_{\rho y}\pi y}{L}\right) + \rho_0\right]^3} - \frac{a_{\rho y}^2\pi^2 k\rho_y}{L^2 R}\cos\left(\frac{a_{\rho y}\pi y}{L}\right)\frac{\left[p_x \cos\left(\frac{a_{px}\pi x}{L}\right) + p_y \sin\left(\frac{a_{py}\pi y}{L}\right) + p_0\right]}{\left[\rho_x \sin\left(\frac{a_{\rho x}\pi x}{L}\right) + \rho_y \cos\left(\frac{a_{\rho y}\pi y}{L}\right) + \rho_0\right]^2} \\
& + \frac{4a_{ux}^2\pi^2\mu u_x}{3L^2}\sin\left(\frac{a_{ux}\pi x}{L}\right)\left[u_x \sin\left(\frac{a_{ux}\pi x}{L}\right) + u_y \cos\left(\frac{a_{uy}\pi y}{L}\right) + u_0\right] - \frac{4a_{ux}^2\pi^2\mu u_x^2}{3L^2}\cos^2\left(\frac{a_{ux}\pi x}{L}\right) \\
& + \frac{a_{uy}^2\pi^2\mu u_y}{L^2}\cos\left(\frac{a_{uy}\pi y}{L}\right)\left[u_x \sin\left(\frac{a_{ux}\pi x}{L}\right) + u_y \cos\left(\frac{a_{uy}\pi y}{L}\right) + u_0\right] - \frac{a_{uy}^2\pi^2\mu u_y^2}{L^2}\sin^2\left(\frac{a_{uy}\pi y}{L}\right) \\
& + \frac{a_{vx}^2\pi^2\mu v_x}{L^2}\cos\left(\frac{a_{vx}\pi x}{L}\right)\left[v_x \cos\left(\frac{a_{vx}\pi x}{L}\right) + v_y \sin\left(\frac{a_{vy}\pi y}{L}\right) + v_0\right] - \frac{a_{vx}^2\pi^2\mu v_x^2}{L^2}\sin^2\left(\frac{a_{vx}\pi x}{L}\right) \\
& + \frac{4a_{vy}^2\pi^2\mu v_y}{3L^2}\sin\left(\frac{a_{vy}\pi y}{L}\right)\left[v_x \cos\left(\frac{a_{vx}\pi x}{L}\right) + v_y \sin\left(\frac{a_{vy}\pi y}{L}\right) + v_0\right] - \frac{4a_{vy}^2\pi^2\mu v_y^2}{3L^2}\cos^2\left(\frac{a_{vy}\pi y}{L}\right) \\
& - \frac{2a_{px}a_{\rho x}\pi^2 k\, p_x\rho_x}{L^2 R}\frac{\cos\left(\frac{a_{\rho x}\pi x}{L}\right)\sin\left(\frac{a_{px}\pi x}{L}\right)}{\left[\rho_x \sin\left(\frac{a_{\rho x}\pi x}{L}\right) + \rho_y \cos\left(\frac{a_{\rho y}\pi y}{L}\right) + \rho_0\right]^2} - \frac{2a_{py}a_{\rho y}\pi^2 k\, p_y\rho_y}{L^2 R}\frac{\cos\left(\frac{a_{py}\pi y}{L}\right)\sin\left(\frac{a_{\rho y}\pi y}{L}\right)}{\left[\rho_x \sin\left(\frac{a_{\rho x}\pi x}{L}\right) + \rho_y \cos\left(\frac{a_{\rho y}\pi y}{L}\right) + \rho_0\right]^2} \\
& + \frac{4a_{ux}a_{vy}\pi^2\mu u_x v_y}{3L^2}\cos\left(\frac{a_{ux}\pi x}{L}\right)\cos\left(\frac{a_{vy}\pi y}{L}\right) - \frac{2a_{uy}a_{vx}\pi^2\mu u_y v_x}{L^2}\sin\left(\frac{a_{uy}\pi y}{L}\right)\sin\left(\frac{a_{vx}\pi x}{L}\right)
\end{aligned}
$$

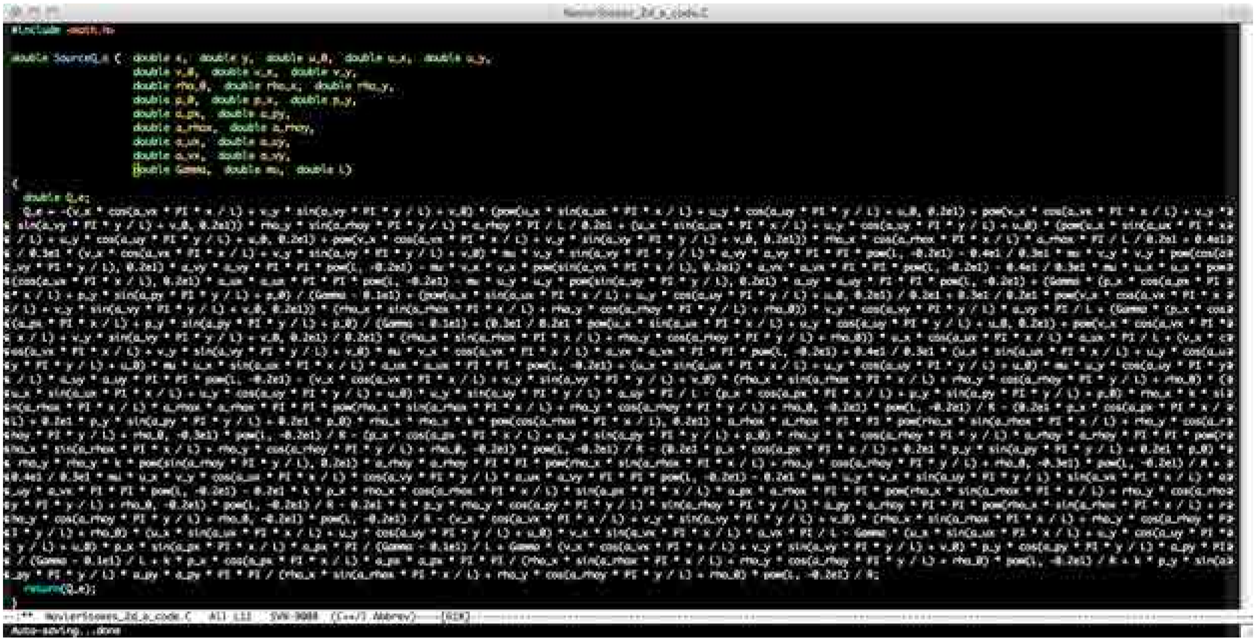

Spalart-Allmaras Perfect-Gas Verification

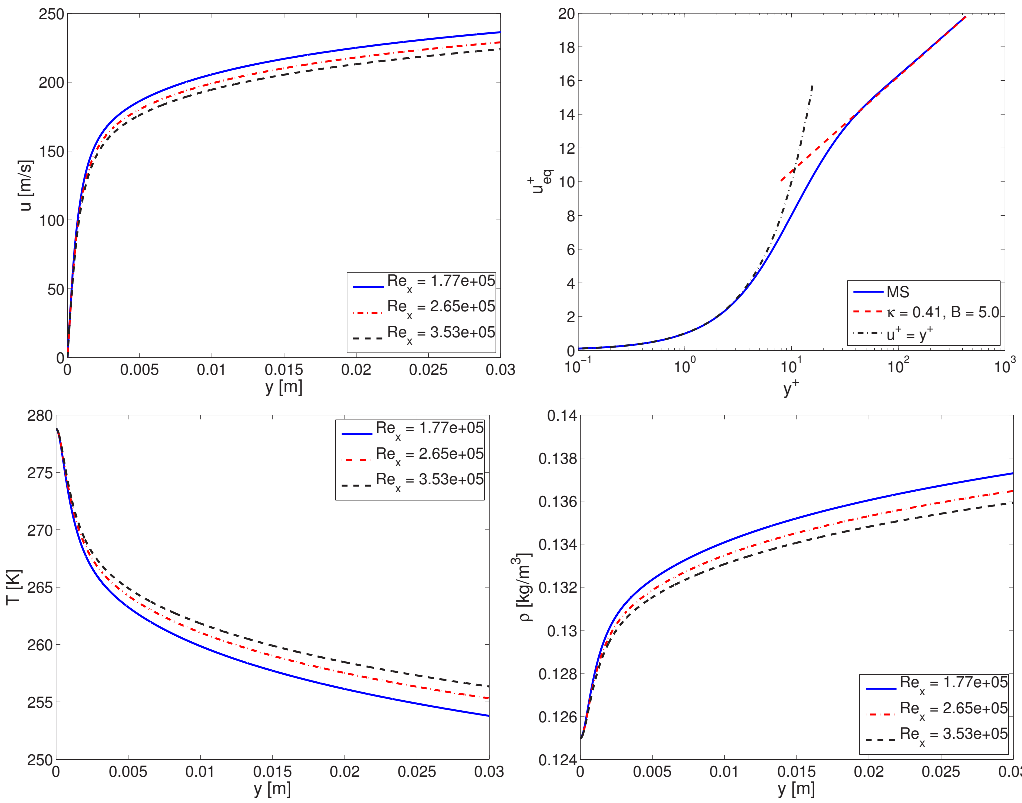

Spalart-Allmaras Perfect-Gas Verification

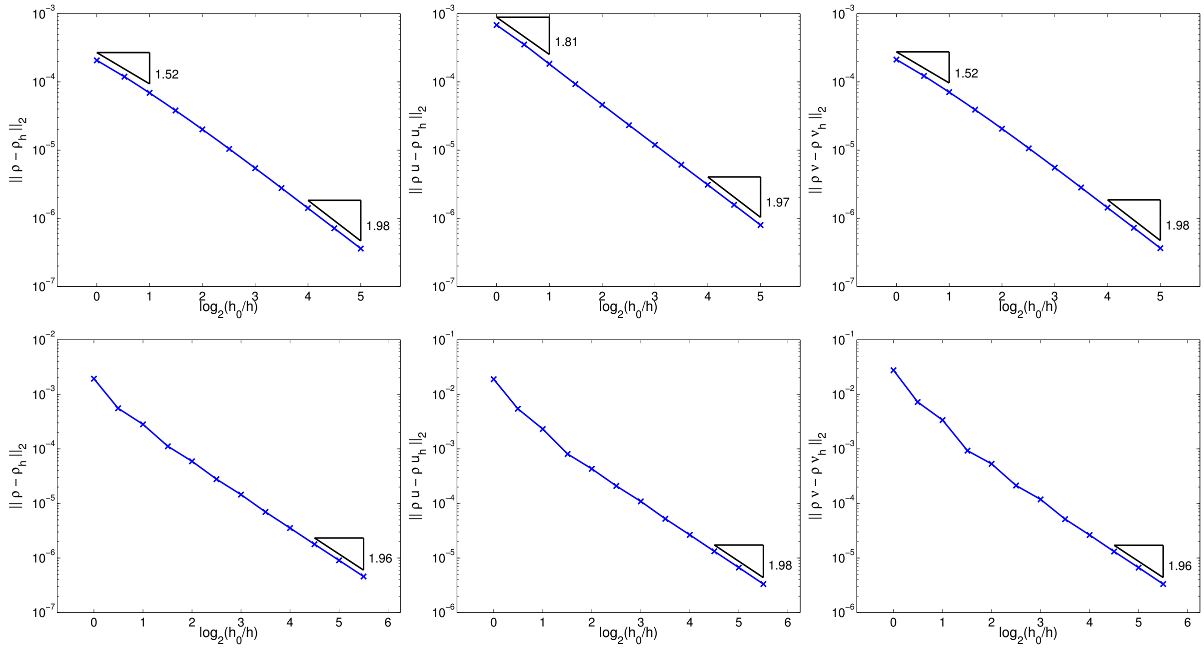

$\bar{\rho}$ $\bar{\rho}\tilde{u}$ $\bar{\rho}\nu_{sa}$

https://red.ices.utexas.edu/projects/software/wiki/MASA

Need for Parallelism

Large Problem Size

- Large numbers of unknowns.
  - For a Lagrange nodal basis:

$$\#\,\text{DOFS} = (\text{NS} + \text{NDIM} + \text{NE} + \text{NT}) \times \#\,\text{NODES}$$

  - Specifically, for our 13 species ablation model in 2D with turbulence

$$\#\,\text{DOFS} = (13 + 2 + 2 + 1) \times \#\,\text{NODES}$$

- For our implicit scheme, both storage and computational cost scale like $(\#\,\text{DOFS})^2$

Need for Parallelism

Complex Physical Models

- Chemical Kinetics, transport properties for NS species inherently expensive.
- Temperature is a nonlinear function of species concentration, internal energy for a mixture of thermally perfect gases.
- Quasi-steady ablation boundary condition is also nontrivial.

Opportunities for Parallelism

Multiple Types of Parallelism

1. **Domain Decomposition:** We use a standard non-overlapping domain decomposition approach provided by `libMesh`. Local computations are perfectly parallel, and the resulting implicit system is solved using preconditioned Krylov solvers from PETSc.
2. **Multithreaded Computation:** The relatively large element matrices resulting for reacting flows are well suited for threaded assembly. `libMesh` provides a convenient interface to Intel's Threading Building Blocks which can provide further parallelization on multicore architectures.
3. **Vectorization:** Remember vectorization? While no longer the *de facto* paradigm for high-performance computing, modern microprocessors offer vectorized instructions worth exploiting. We are using Eigen for dense linear algebra and inherit its SSE optimizations.

Domain Decomposition

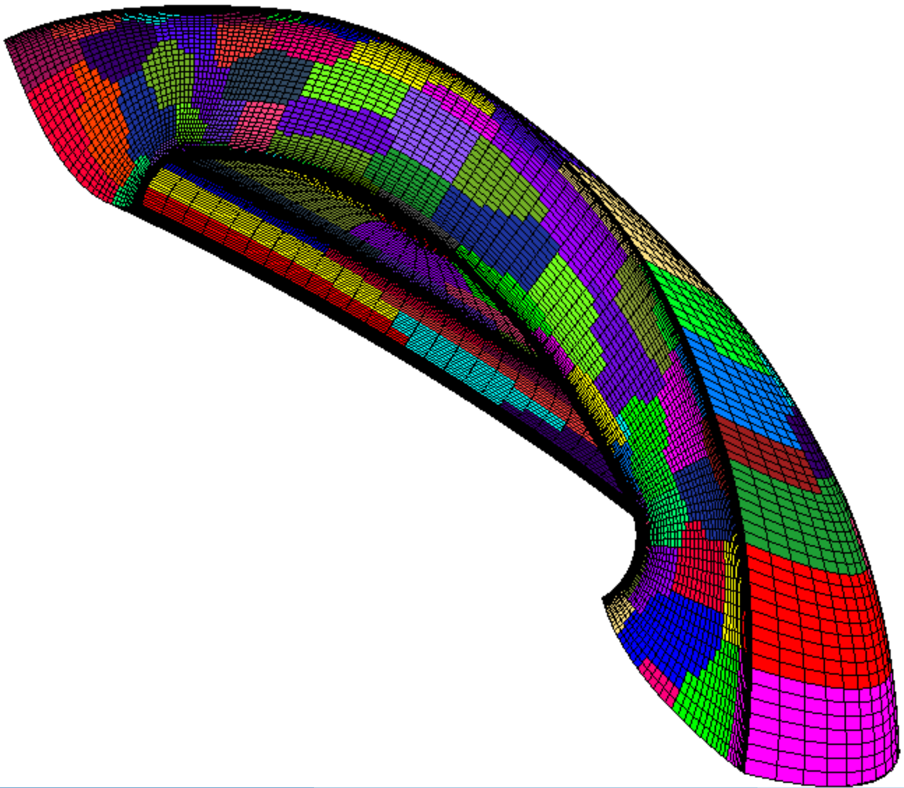

Domain Decomposition

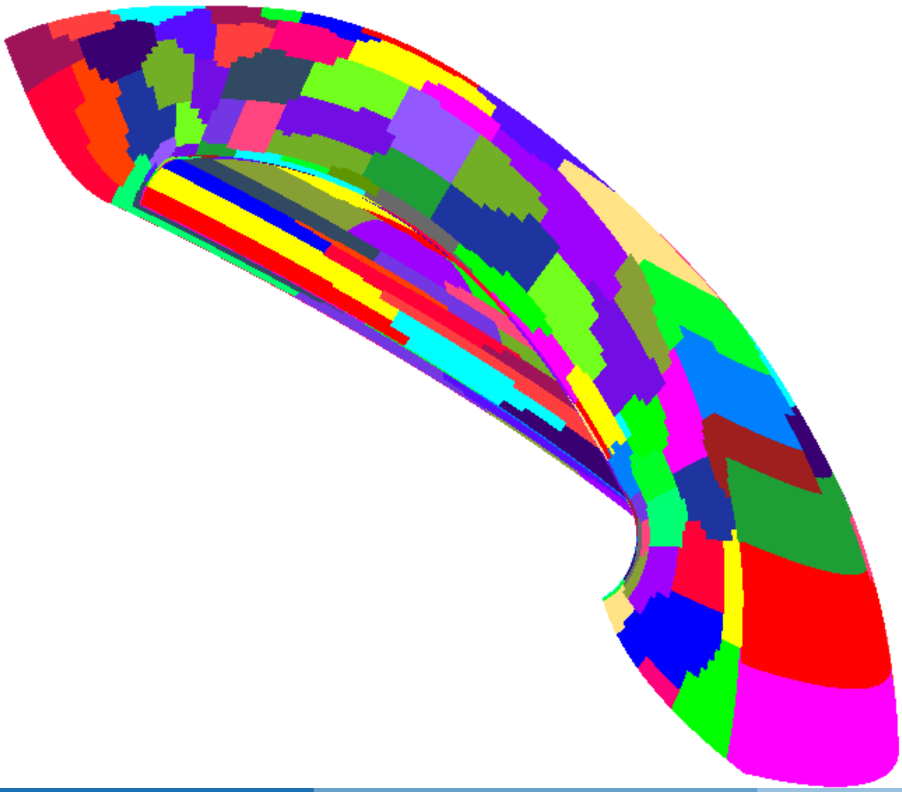

Speedup – Domain Decomposition

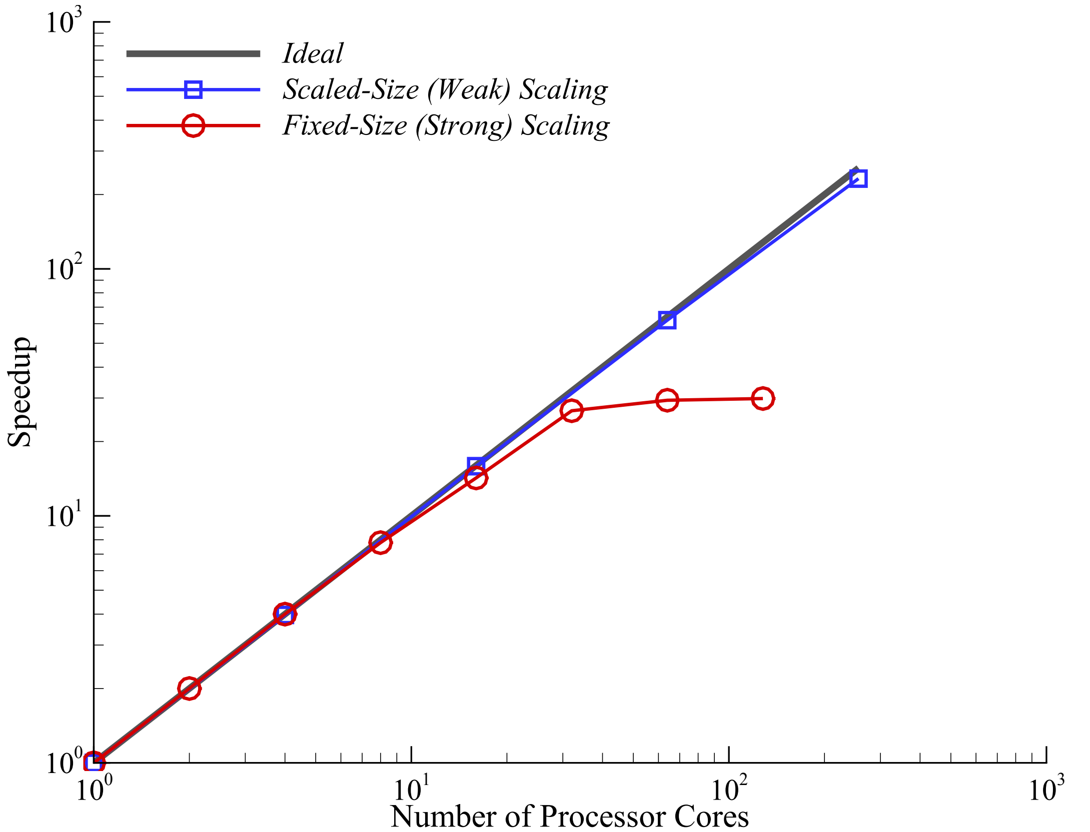

Multithreading

- Modern Parallel systems often contain 12–16 (or more) on-node cores connected via low-latency network.
- On-node multithreading allows an additional parallel mechanism that can extend scalability in certain circumstances.
- `libMesh` provides a clean interface to Intel®'s Threading Building Blocks (TBB) which is we have access to.
- TBB is a C++ template library consisting of
  - Algorithms
  - Containers
  - Mutexes
  - Timing routines
  - Memory allocators

  designed to help avoid low-level use of platform-specific (e.g. `pthread`) implementations.

Intel®'s Threading Building Blocks

- Requires more work than OpenMP but
  - Has better type-safety
  - Easier to reuse code
  - More natural for use with C++
- Once a standard `for` loop is selected for parallelization its components are abstracted as C++ `Range` and `Body` objects
- In FIN-S we parallelize matrix assembly, primitive variable computation, and other operations in this way.
  - Some operations perfectly asynchronous – e.g. computing primitive variables.
  - Other operations require locking shared objects – e.g. inserting local contributions to a global matrix.
  - Special care needed when interfacing with 3rd party libraries.

Speedup – Multithreading

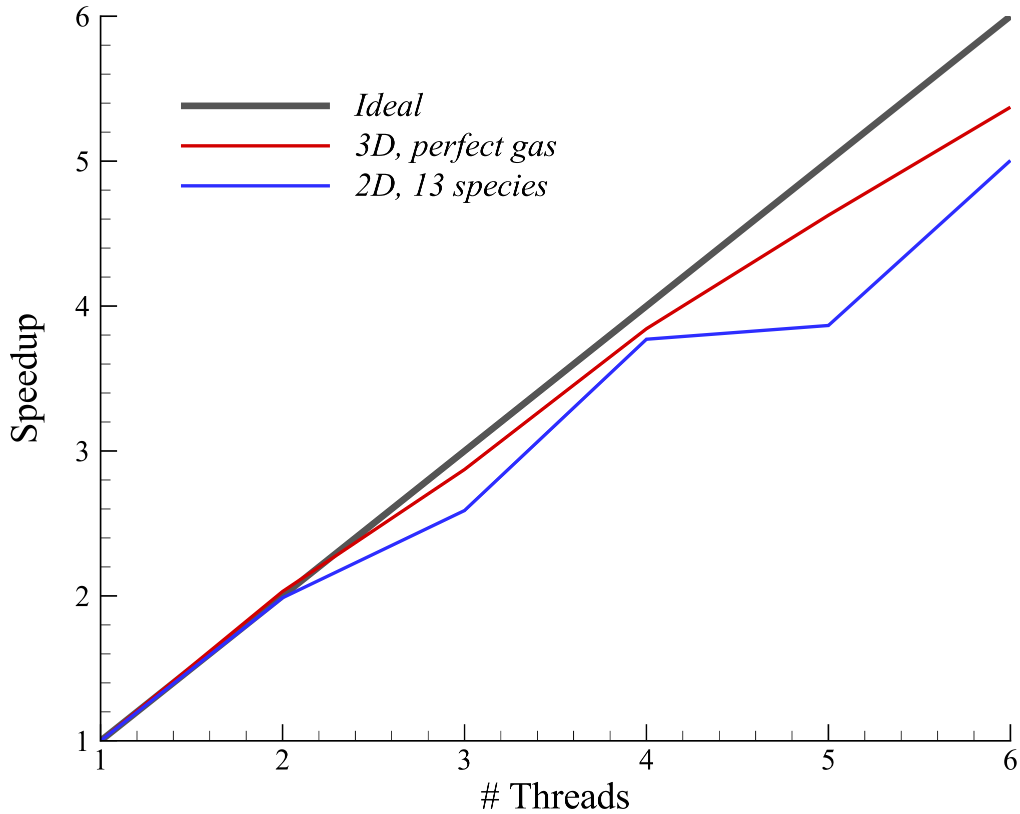

Background – AEDC Sharp Double Cone

- A sharp 25°–55° double cone was tested in N_2 at CUBRC.
- It was discovered that freestream vibrational nonequilibrium must be properly modeled for CFD to match experiment (Nompelis & Candler).
- The AEDC Hypervelocity Wind Tunnel No. 9 also uses N_2 as its test gas.
- A series of tests were conducted at AEDC using the same model to investigate the presence of vibrational nonequilibrium in the freestream.

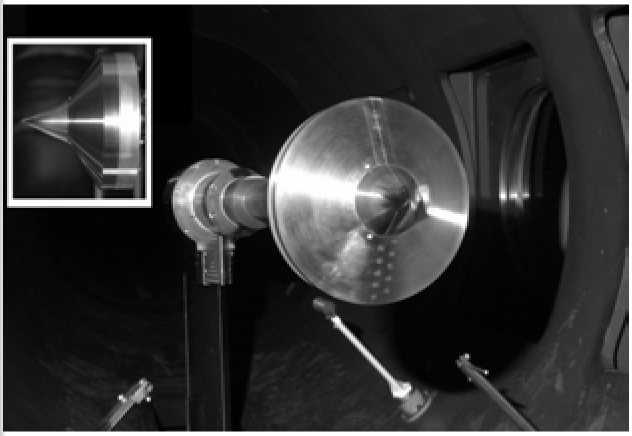

Observations

- Four Reynolds numbers were tested in the nominally Mach 14 nozzle.

Run	2890	2891	2893	2894	
M_∞	13.6	13.17	12.73	12.63	
Re_D	1.12×10^6	4.11×10^5	8.44×10^4	5.86×10^4	
ρ_∞	7.81×10^{-3}	2.96×10^{-3}	5.90×10^{-4}	3.98×10^{-4}	kg/m^3
U_∞	2006.6	1949.8	1763.5	1682.6	m/sec
T_∞	52.3	52.7	46.1	42.7	K

- No appreciable vibrational nonequilibrium effects observed.
- Highly unsteady flow observed for *all* Reynolds numbers tested.
- For a uniform freestream, CFD predicts steady flow for the two lowest Reynolds numbers.

Steady states, runs 2893 and 2894

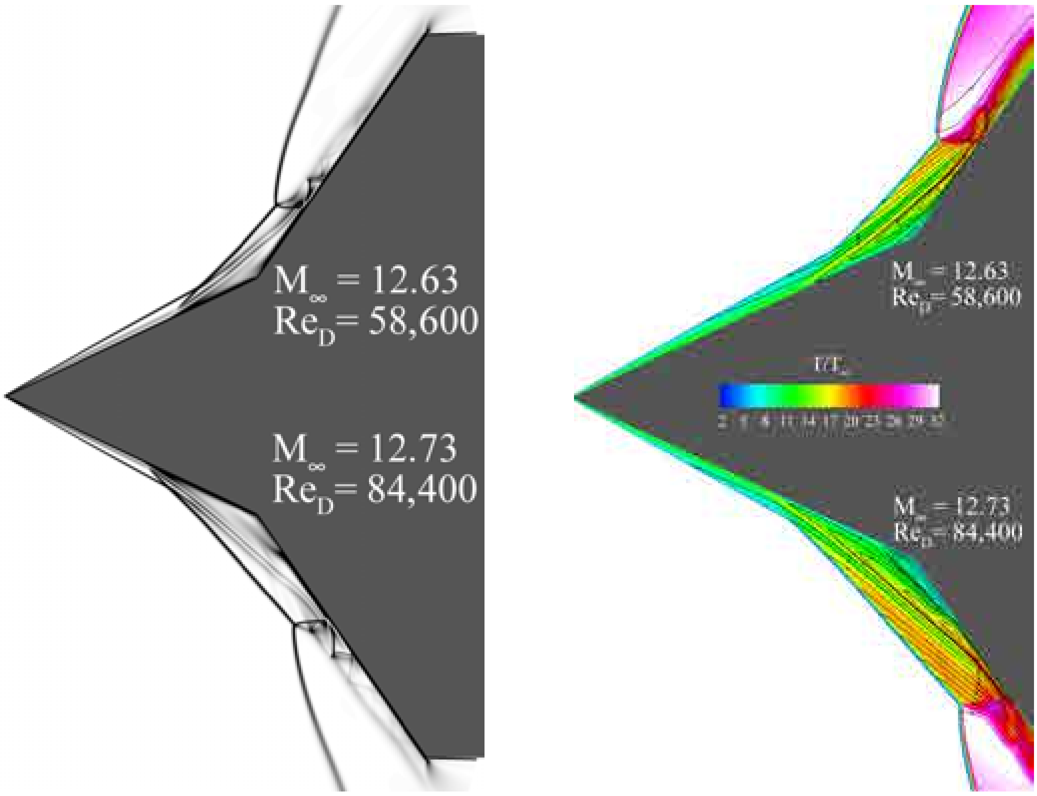

Time Convergence, run 2894

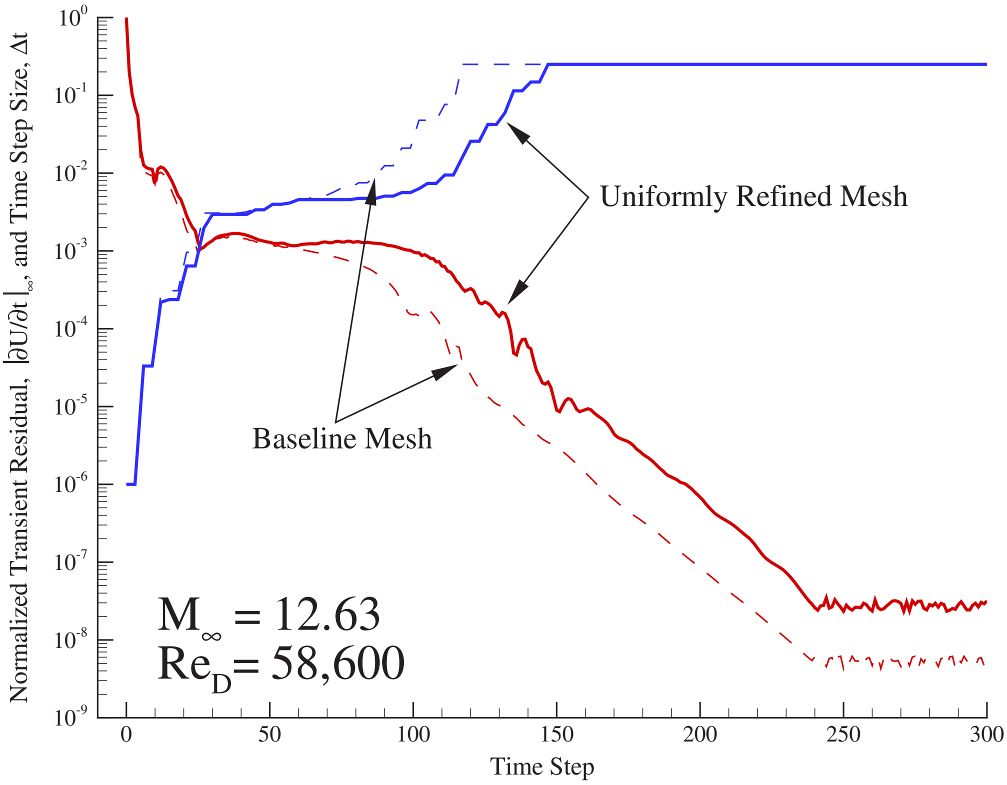

High speed schlieren, run 2890

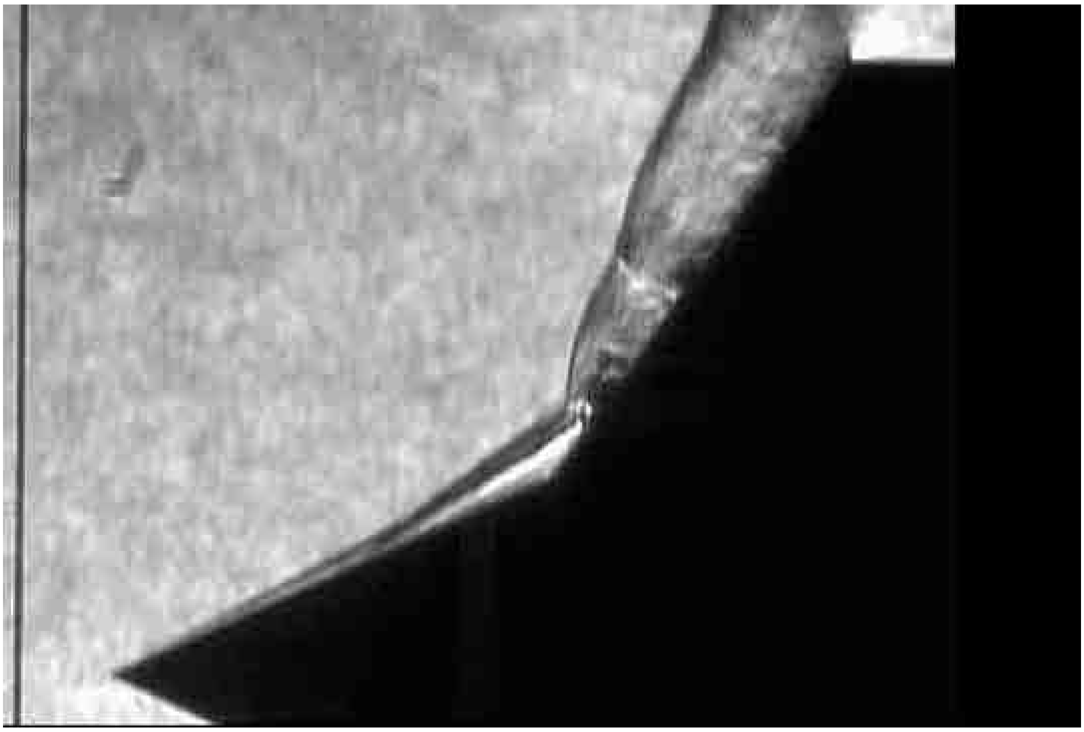

Computed schlieren, run 2890

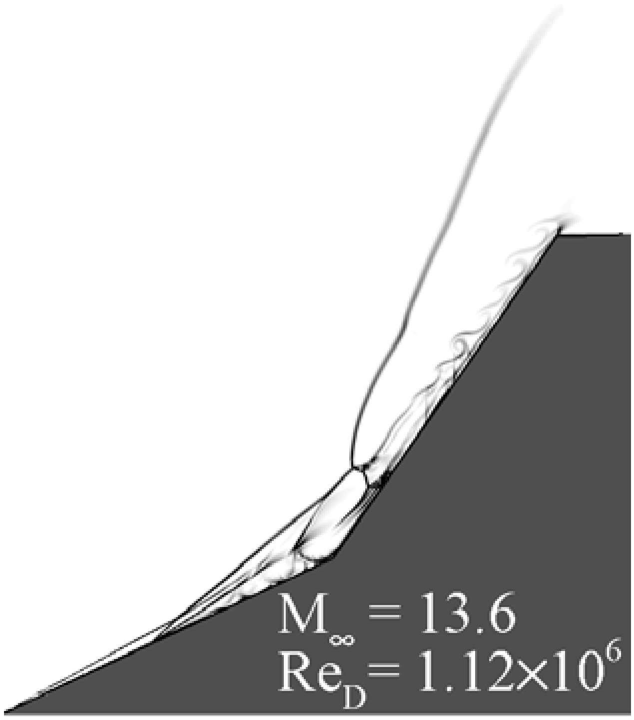

Possible Mechanism for Observed Unsteadiness

- For a uniform inflow, CFD converges to a steady–state for the two lowest Reynolds numbers tested.
- This is in contrast to the experimental results.
- My conjecture is that freestream noise drives the unsteady behavior at these low Reynolds number.
- Remaining analysis is focused on testing this theory.

Noise Characterization

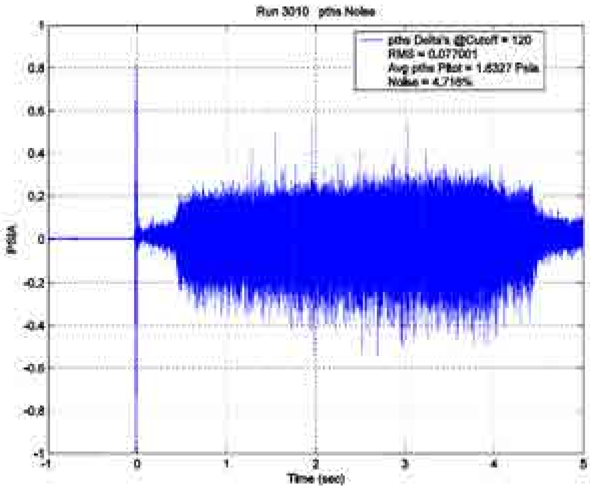

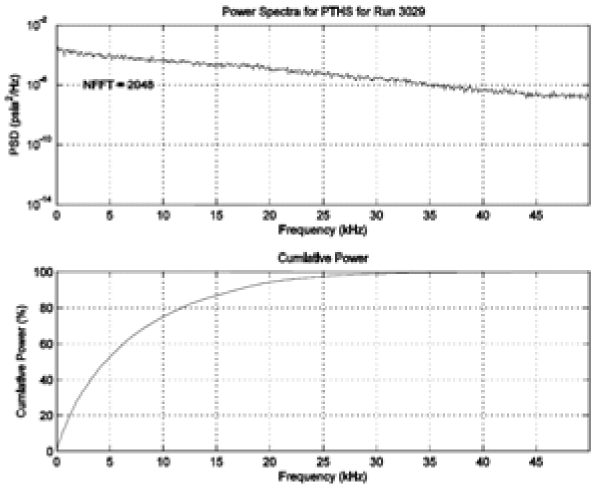

Noise Characterization

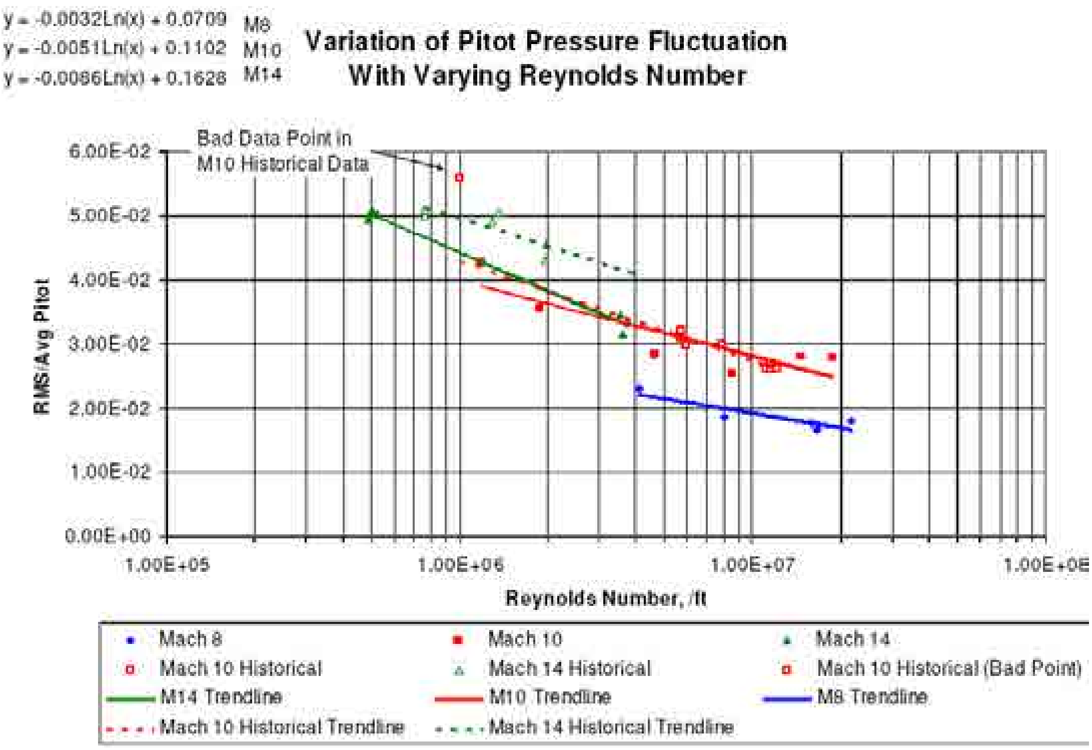

Results – Flowfield

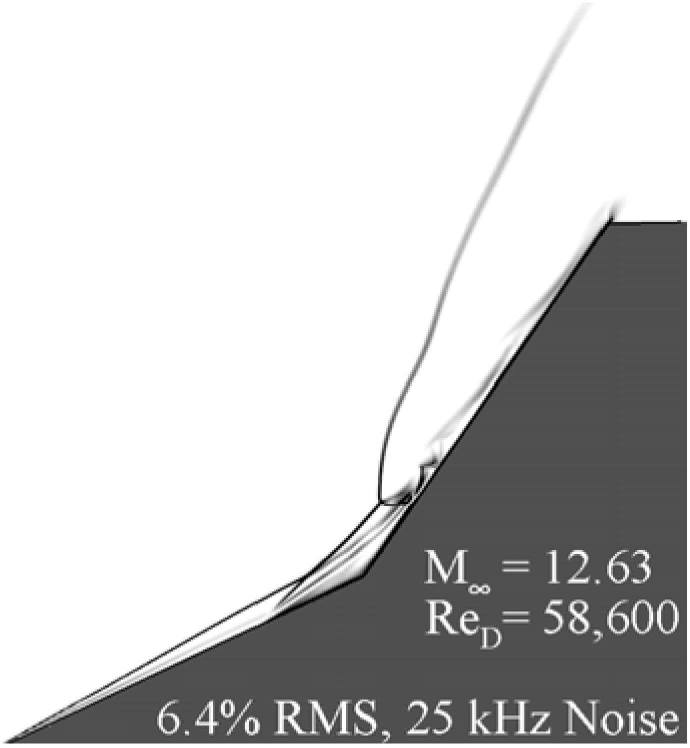

Results | Perfect Gas Flow over a Double Cone

Results – Surface Pressure

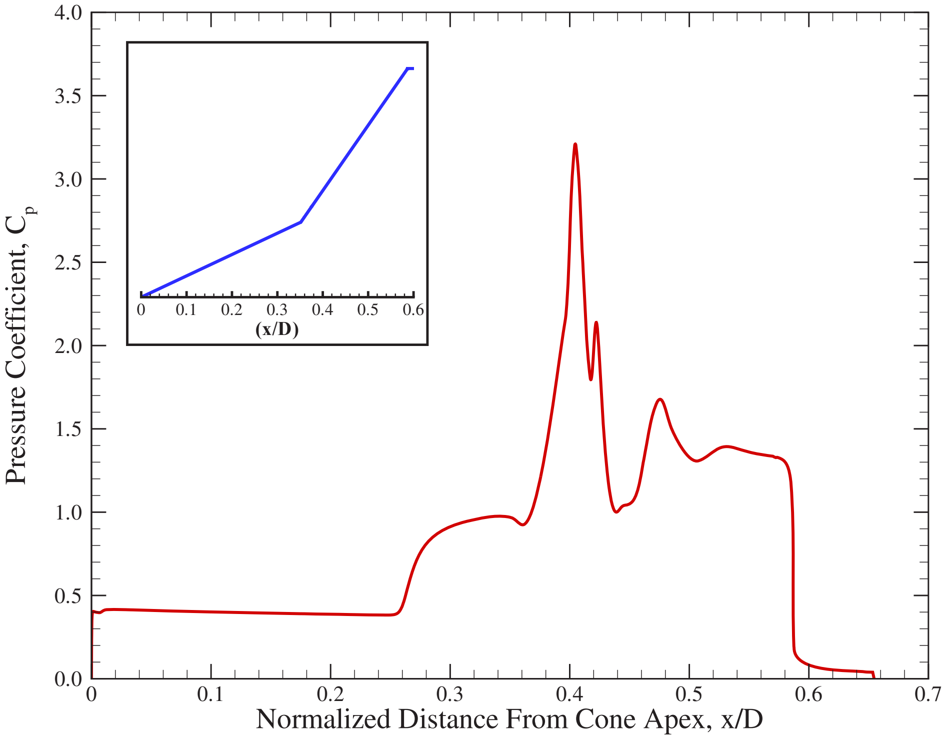

25 kHz, 6% RMS Pitot Pressure Fluctuation

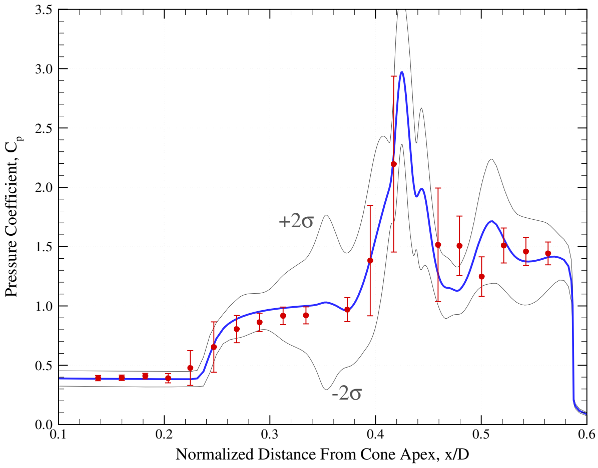

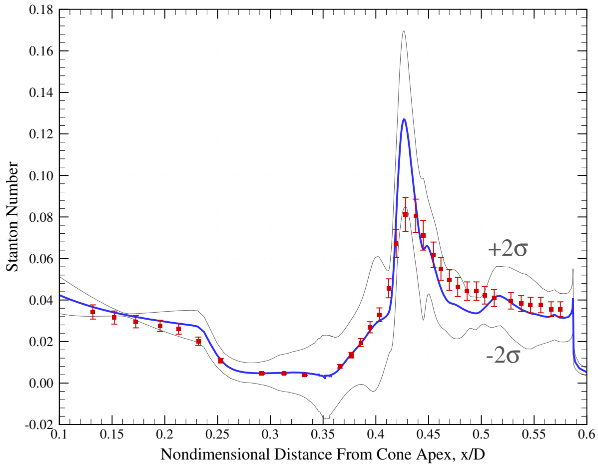

Frequency Influence

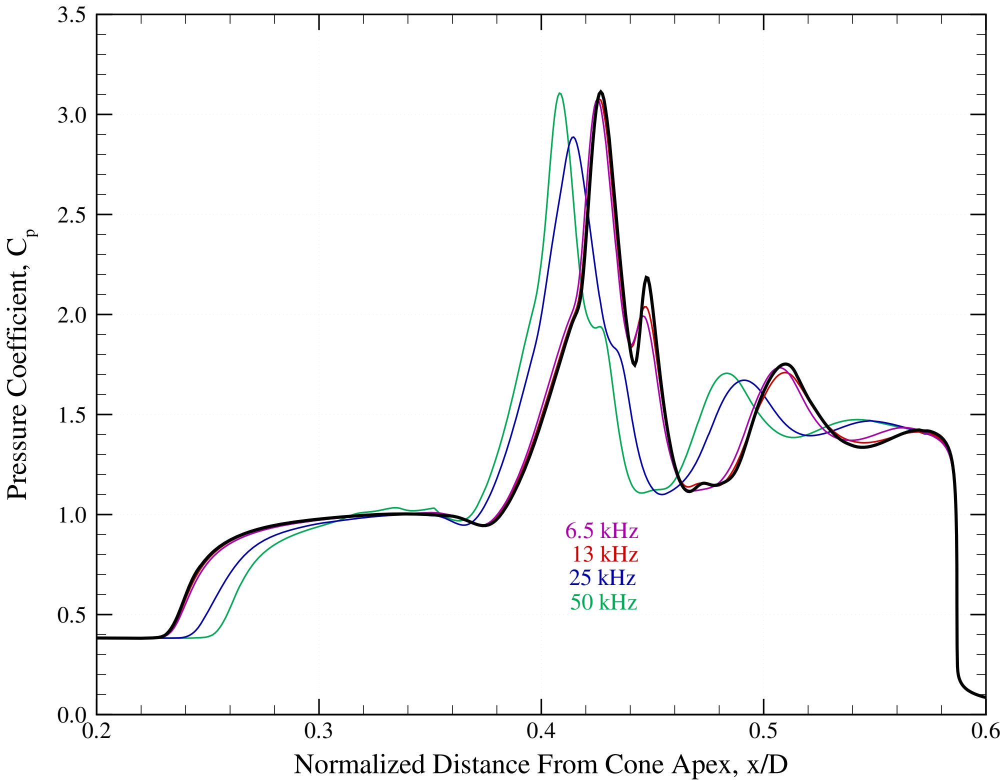

2D Extended Cylinder

- Laminar flow in thermal equilibrium
- Chemical nonequilibrium, 5 species air (N_2, O_2, NO, N, O)
- 5 reaction model with Park 1990 rates

$$
\begin{aligned}
cN_{2,\infty} &= 0.78, cO_{2,\infty} = 0.22 \\
U_\infty &= 6,731 \ ^{\mathrm{m}}/_{\mathrm{sec}} \\
\rho_\infty &= 6.81 \times 10^{-4} \ ^{\mathrm{kg}}/_{\mathrm{m}^3} \\
T_\infty &= 265 \mathrm{\ K}
\end{aligned}
$$

- Blottner/Wilke/Eucken with constant Lewis number $Le = 1.4$ for transport properties
- Mesh, iterative convergence
- FIN-S/DPLR comparison

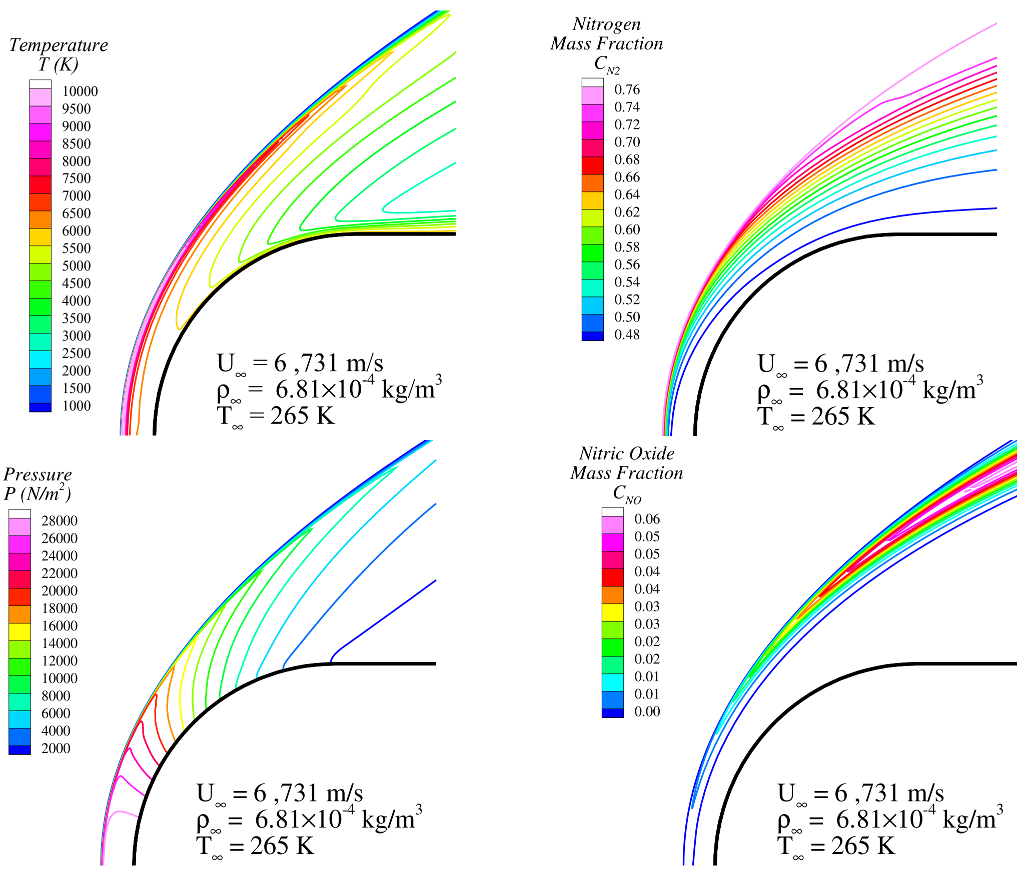

Code-to-Code Comparison – Stagnation Line

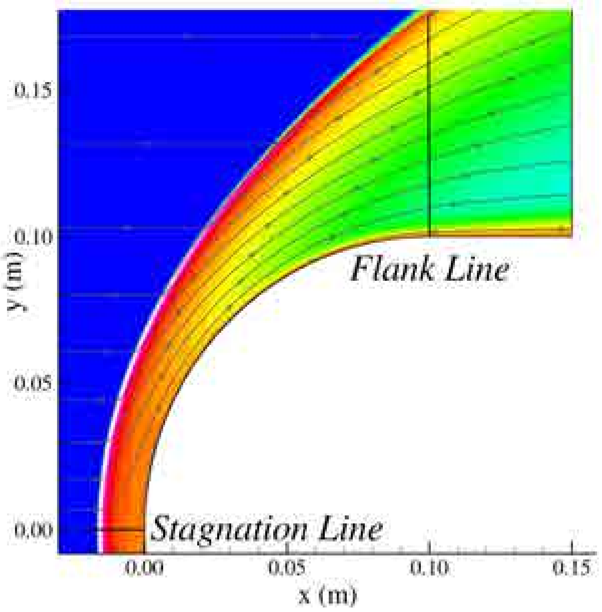

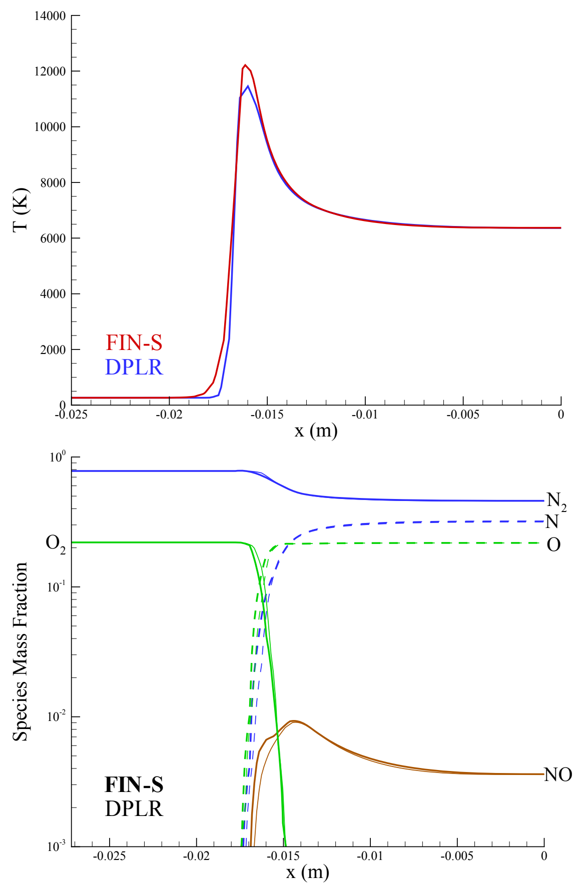

Code-to-Code Comparison – Flank Line

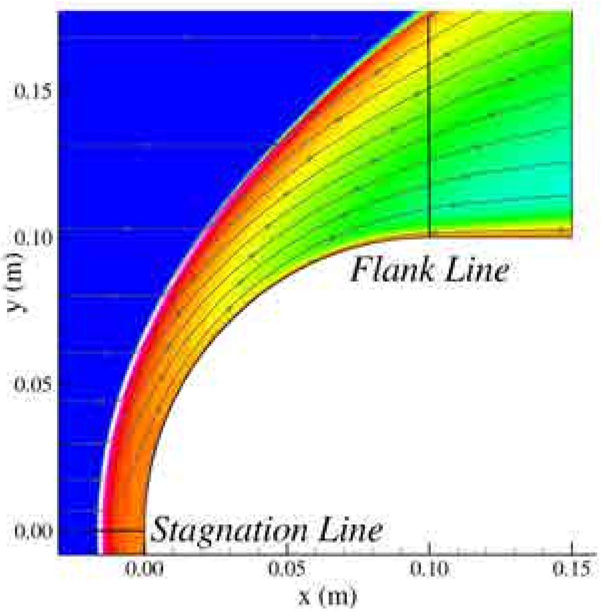

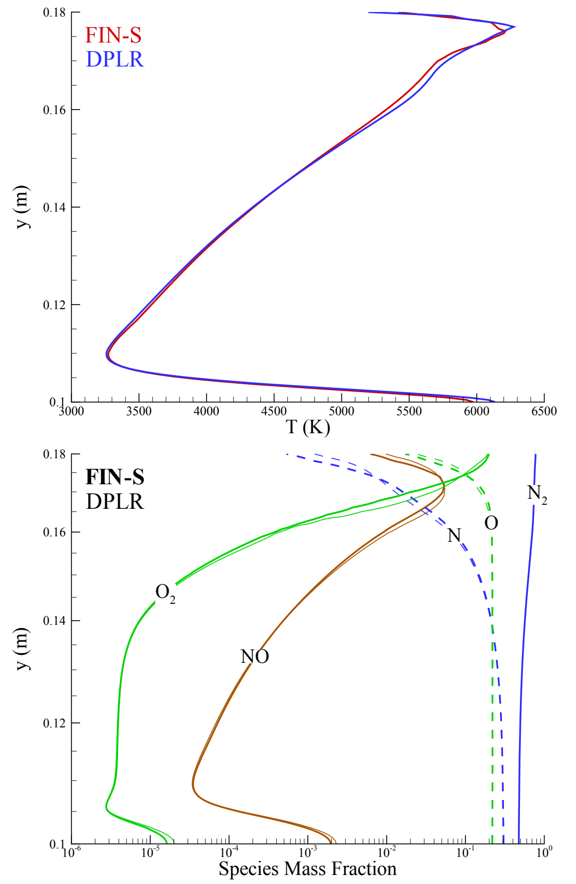

Mesh Convergence

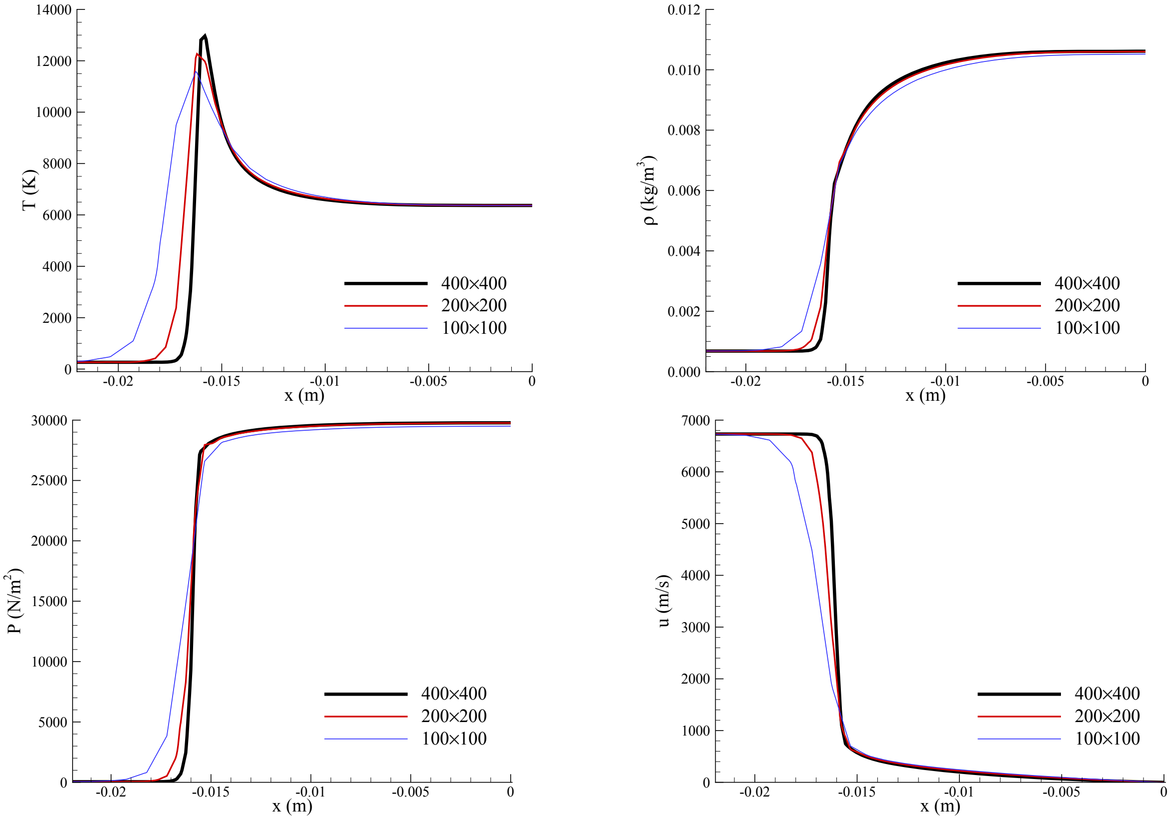

Iterative Convergence

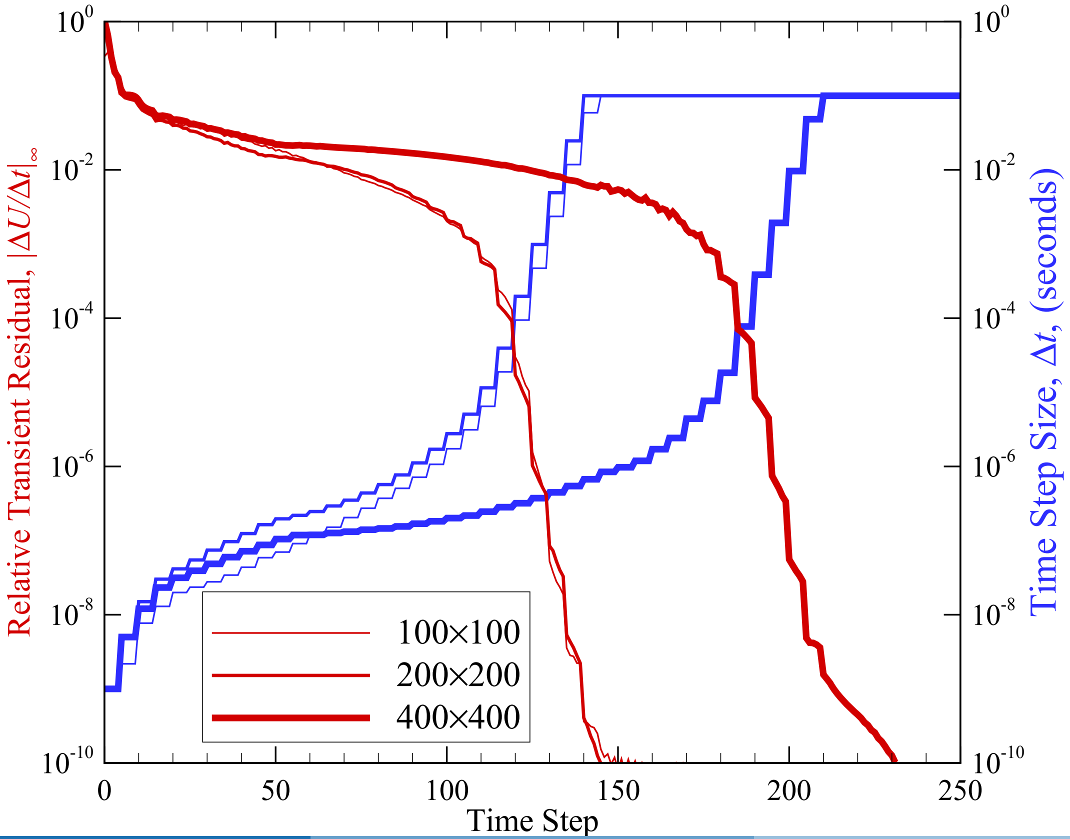

Results | Viscous Reacting Flow with Quasi-Steady Surface Ablation

Ablating Boundary Experiments

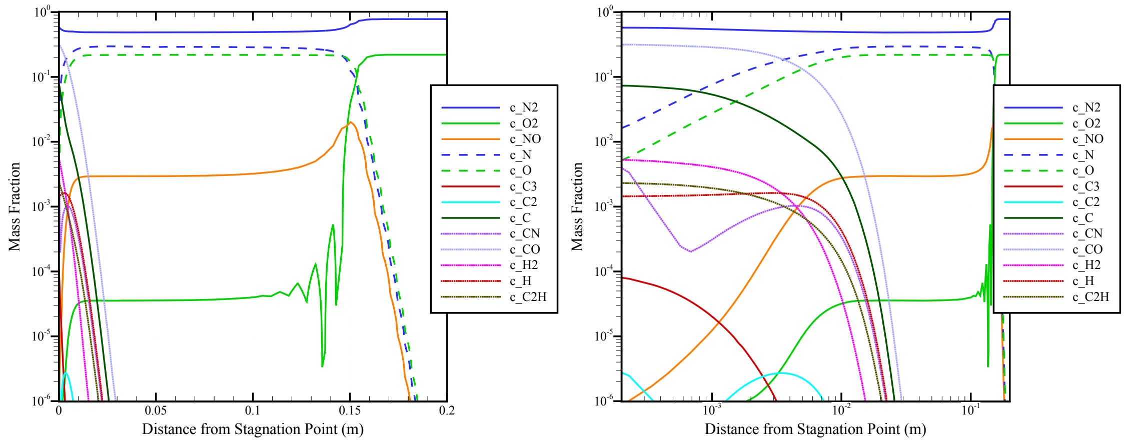

- Turbulent flow in thermochemical nonequilibrium, 13 species air (N_2, O_2, NO, N, O, C_3, C_2, C, CN, CO, H_2, H, C_2H), 18 reaction model with Park 2001 rates
- 5 Meter-scale domain, millimeter-scale chemical boundary layer

Results | Viscous Reacting Flow with Quasi-Steady Surface Ablation

Ablating Boundary Experiments

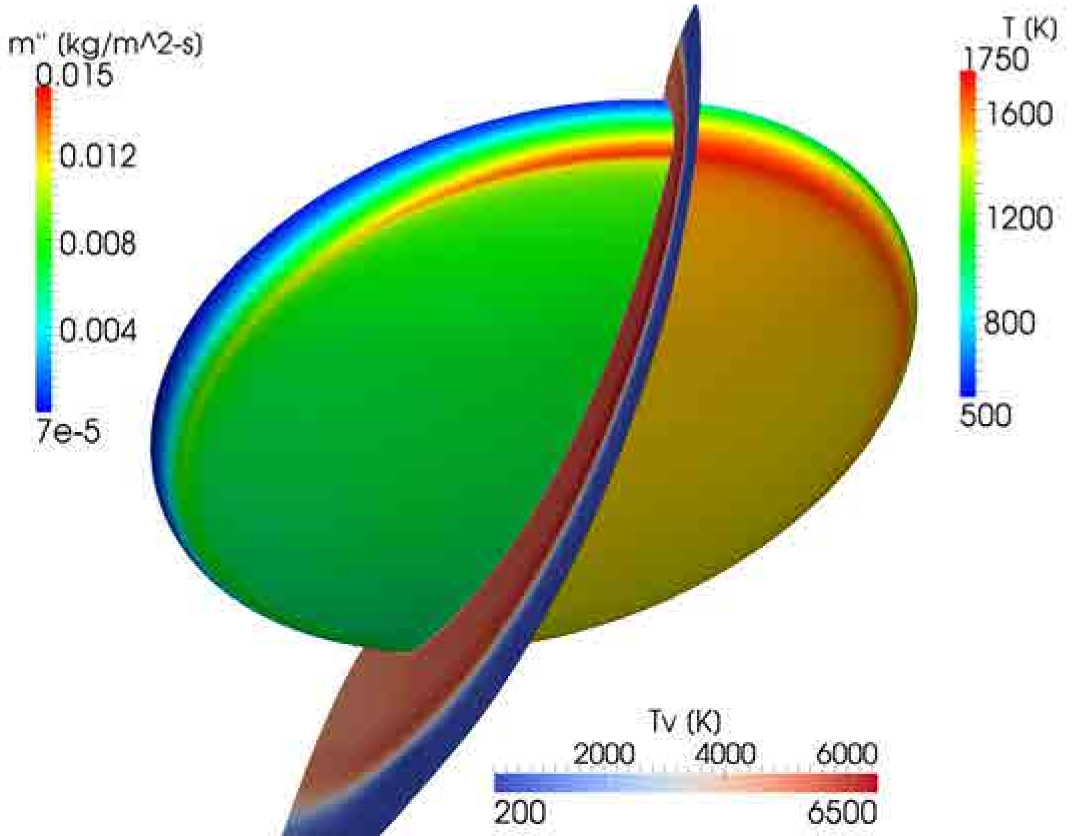

Arcjet Flowfields

Motivation

- Arcjets are uniquely suited to perform high enthalpy, long duration material response testing.
- Modern computational techniques are required to adequately characterize the freestream properties.
- Analysis complicated by multitude of scales, physical phenomenon:
  - Very low speed, high pressure plenum,
  - very high speed, low pressure nozzle exit,
  - highly nonequilibrium flow about test specimen.
- Adequately treating these phenomenon simultaneously is challenging for numerical methods.

Arcjet Flowfields

Arcjet Flowfields

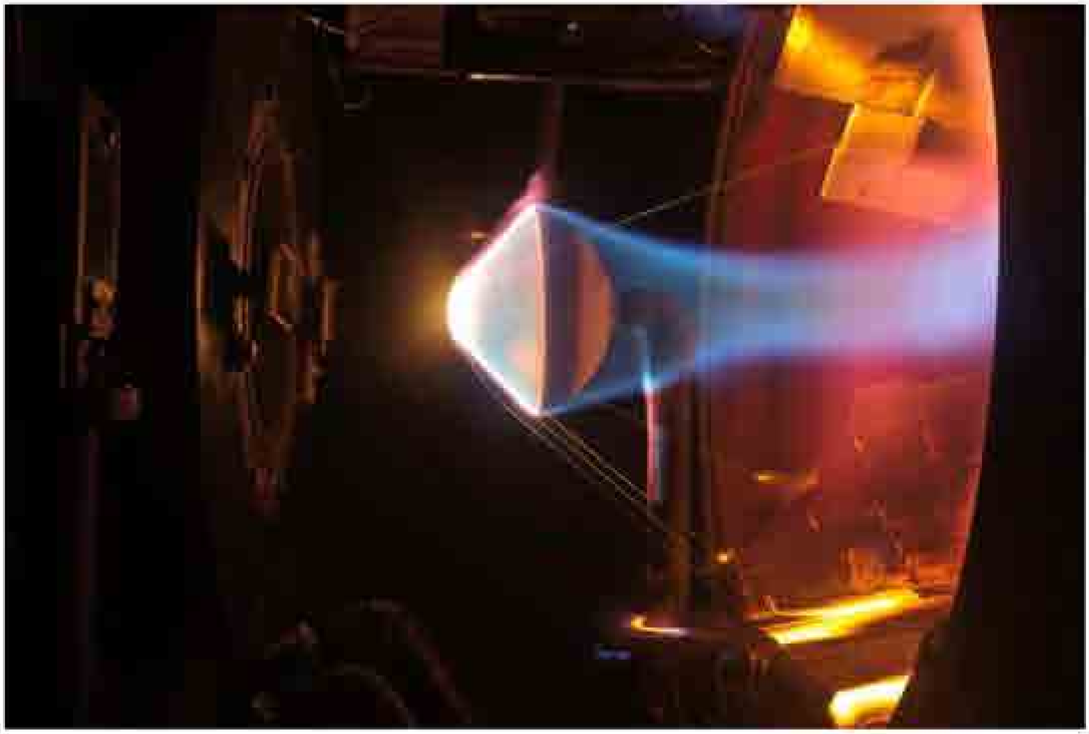

Arcjet Flowfields

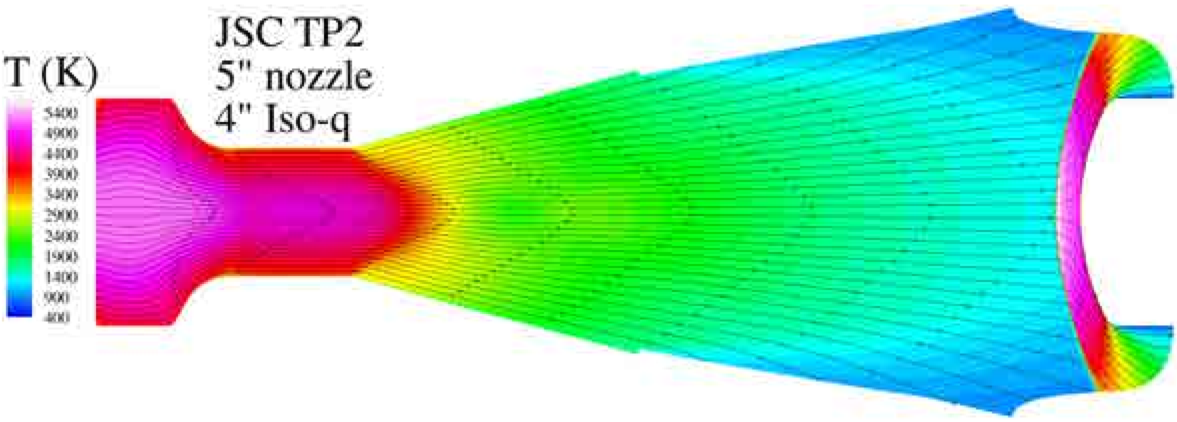

Arcjet Flowfields

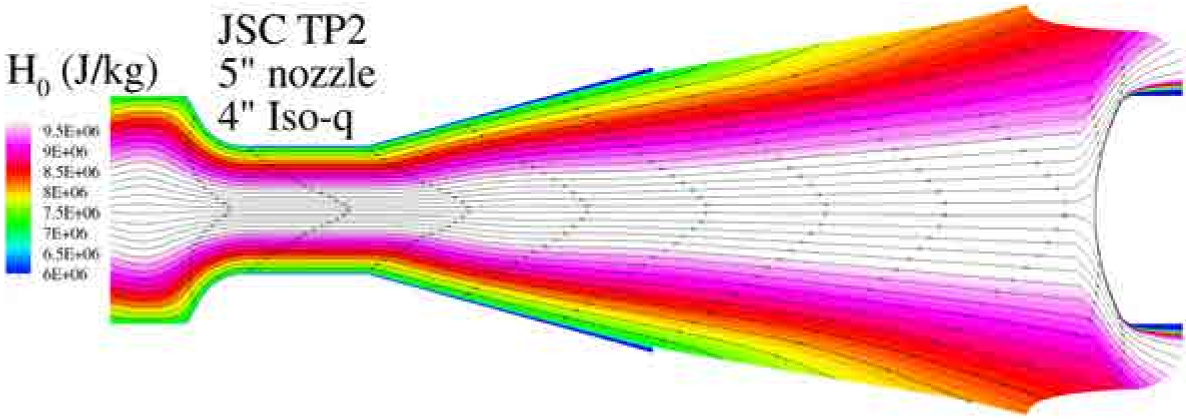

Arcjet Simulations – Enabling Boundary Conditions

Implicit, Characteristic Boundary Conditions for Thermochemical Nonequilibrium Flows

Consider the transformation from conserved variables to characteristic variables:

$$\delta\hat{\boldsymbol{U}} = \frac{\partial\hat{\boldsymbol{U}}}{\partial\boldsymbol{U}}\delta\boldsymbol{U} = \boldsymbol{M}^{-1}\delta\boldsymbol{U}$$

where $\delta\boldsymbol{U}$ is a pertubation in the conserved variables, $\delta\hat{\boldsymbol{U}}$ is a pertubation in the conserved variables, and $\boldsymbol{M}^{-1}$ is the transformation matrix given by the left eigenvectors from the inviscid flux Eigendecomposition for a specified flux direction.

We will manipulate this statement such that outgoing/incoming characteristic variables are unchanged at inflow/outflow boundaries, respectively.

Arcjet Simulations – Enabling Boundary Conditions

Characteristic boundary conditions for reservoir-type boundaries.

Given: H_0, $\{c_s\}$, $\dot{m}_A$, $\hat{\boldsymbol{v}}$, and $\boldsymbol{U}_B$.

Let $\boldsymbol{U} = \boldsymbol{U}_B$ serve as an initial guess.
do
  Form the transformation matrix $\boldsymbol{M}^{-1} = \boldsymbol{M}^{-1}(\boldsymbol{U})$
  Define the outgoing conserved variable increment $\delta\boldsymbol{U}^{+} = \boldsymbol{U} - \boldsymbol{U}_B$
  Compute the outgoing characteristics increment $\delta\hat{\boldsymbol{U}}^{+} = \boldsymbol{M}^{-1}\delta\boldsymbol{U}^{+}$
  Define the unconstrained residual $\boldsymbol{r} = -\delta\hat{\boldsymbol{U}}$
  For each incoming characteristic, replace a row of $\boldsymbol{M}^{-1}$ and $\boldsymbol{r}$ with a
  linearized constraint derived from the reservoir conditions.
  Solve for the increment $\boldsymbol{M}^{-1}\delta\boldsymbol{U} \equiv -\boldsymbol{r} = -\delta\hat{\boldsymbol{U}}$
  Update the iterate $\boldsymbol{U} \leftarrow \boldsymbol{U} + \delta\boldsymbol{U}$
while $\|\delta\boldsymbol{U}\|_\infty > \varepsilon_{it}$
Compute $\boldsymbol{F} = \boldsymbol{F}(\boldsymbol{U})$ as the inviscid flux on the outflow boundary in the weak statement.

Arcjet Simulations – Enabling Boundary Conditions

Characteristic boundary conditions for vacuum-type boundaries.

Given: $\boldsymbol{U}_B$ and $\mathrm{P}_{\mathrm{back}} = \{\text{vacuum fraction}\}\times\mathrm{P}_{\mathrm{exit}}$.

Let $\boldsymbol{U} = \boldsymbol{U}_B$ serve as an initial guess.
do
  Form the transformation matrix $\boldsymbol{M}^{-1} = \boldsymbol{M}^{-1}(\boldsymbol{U})$
  Define the outgoing conserved variable increment $\delta\boldsymbol{U}^{+} = \boldsymbol{U} - \boldsymbol{U}_B$
  Compute the outgoing characteristics increment $\delta\hat{\boldsymbol{U}}^{+} = \boldsymbol{M}^{-1}\delta\boldsymbol{U}^{+}$
  Define the unconstrained residual $\boldsymbol{r} = -\delta\hat{\boldsymbol{U}}$
  For the single incoming characteristic, replace the row of $\boldsymbol{M}^{-1}$ and $\boldsymbol{r}$ with a
  linearized constraint derived from the back pressure condition.
  Solve for the increment $\boldsymbol{M}^{-1}\delta\boldsymbol{U} \equiv -\boldsymbol{r} = -\delta\hat{\boldsymbol{U}}$
  Update the iterate $\boldsymbol{U} \leftarrow \boldsymbol{U} + \delta\boldsymbol{U}$
while $\|\delta\boldsymbol{U}\|_\infty > \varepsilon_{it}$
Compute $\boldsymbol{F} = \boldsymbol{F}(\boldsymbol{U})$ as the inviscid flux on the inflow boundary in the weak statement.

Arcjet Flowfields – NASA Ames AHF, 7in Nozzle

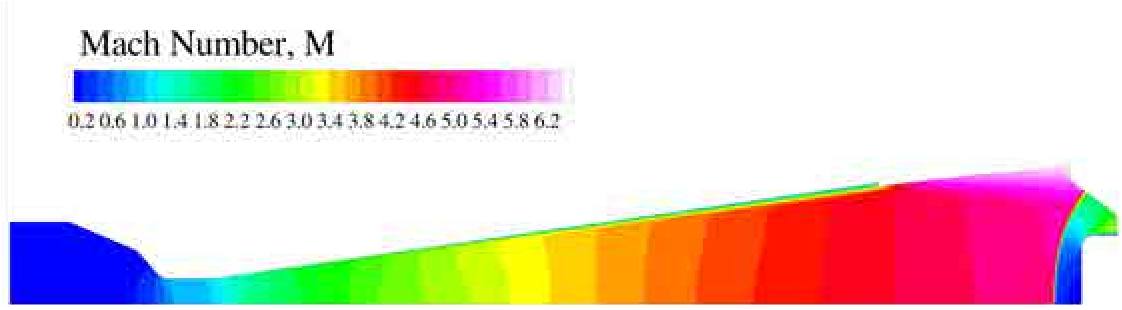

Arcjet Flowfields – NASA Ames AHF, 7in Nozzle

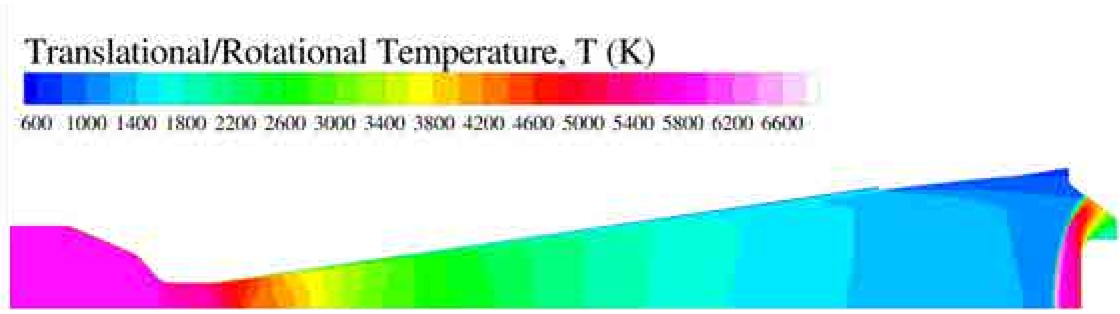

Arcjet Flowfields – NASA Ames AHF, 7in Nozzle

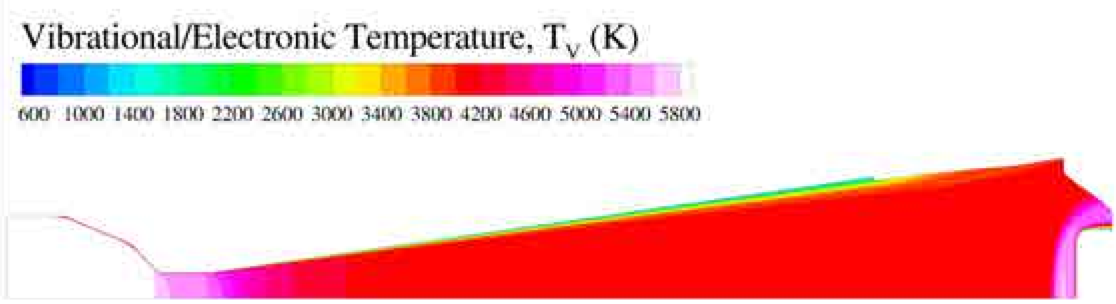

Arcjet Flowfields – NASA Ames AHF, 7in Nozzle

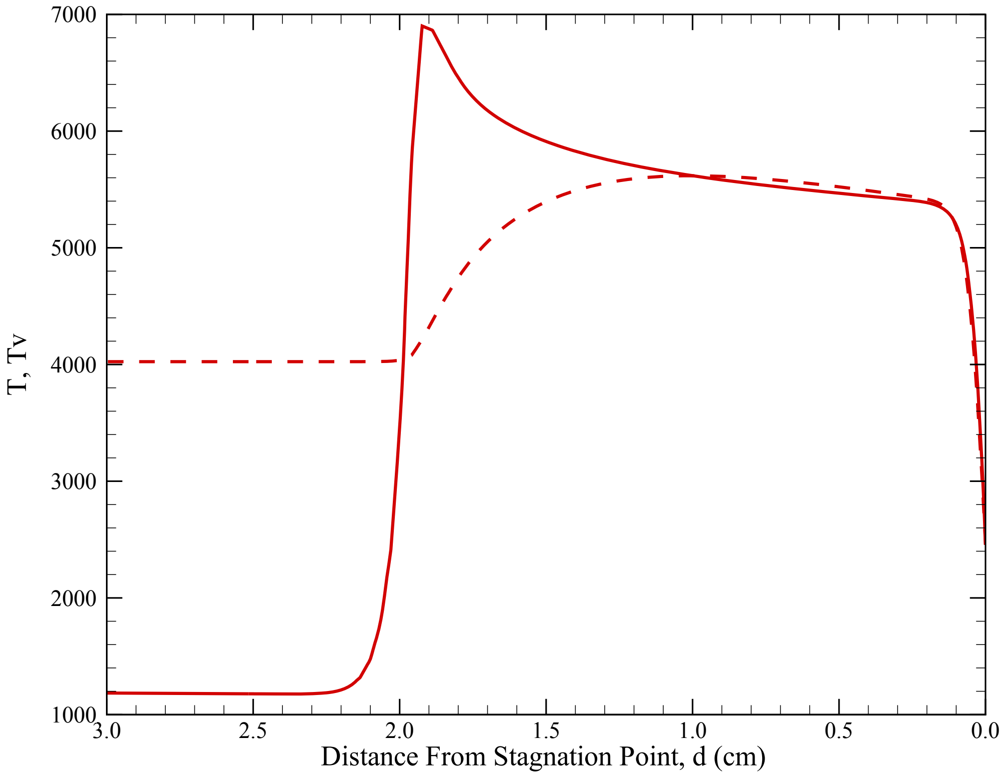

Arcjet Flowfields – NASA Ames AHF, 7in Nozzle

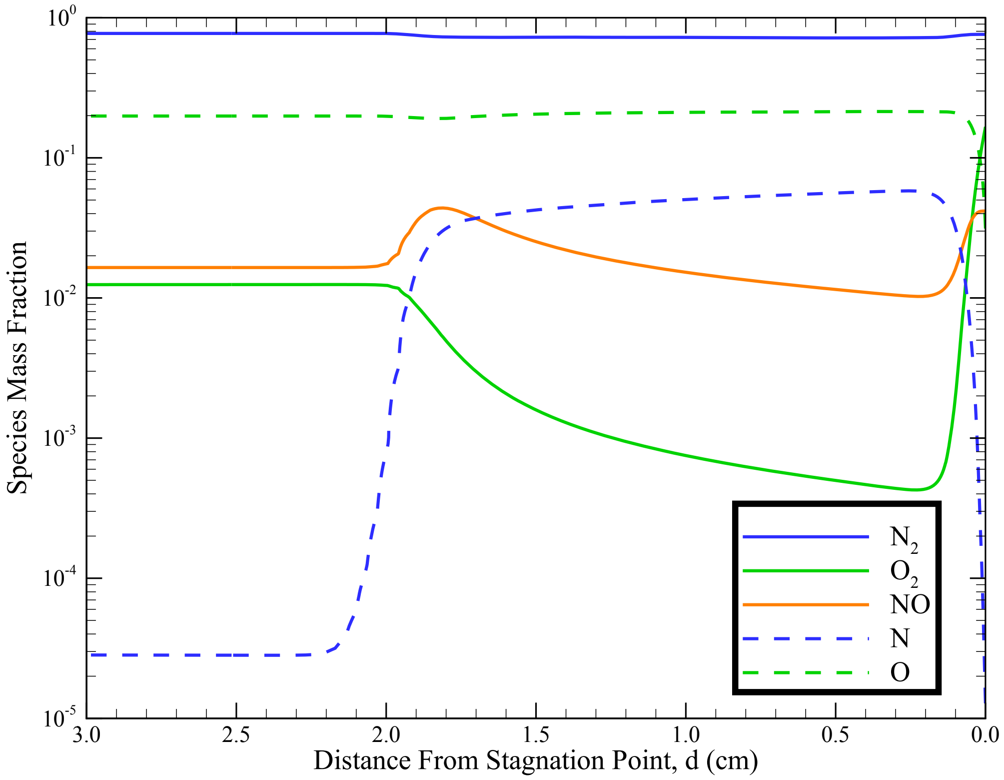

Arcjet Flowfields – NASA Ames AHF, 7in Nozzle

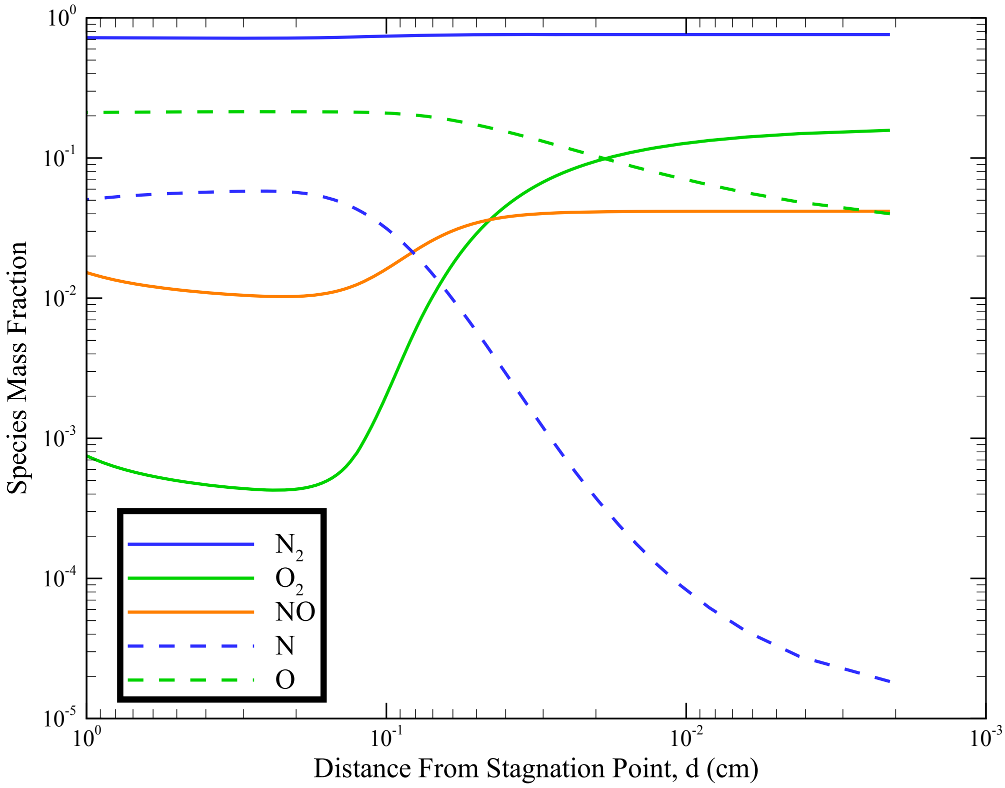

Arcjet Flowfields – NASA Ames AHF, 7in Nozzle

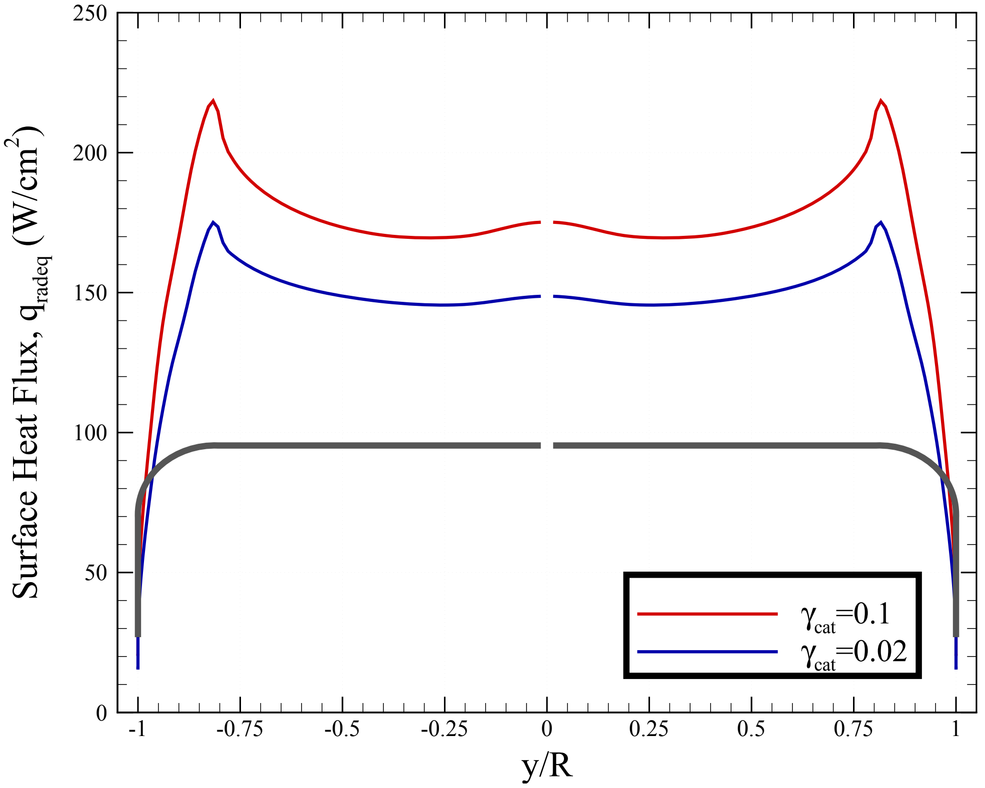

Arcjet Flowfields – NASA Ames AHF, 7in Nozzle

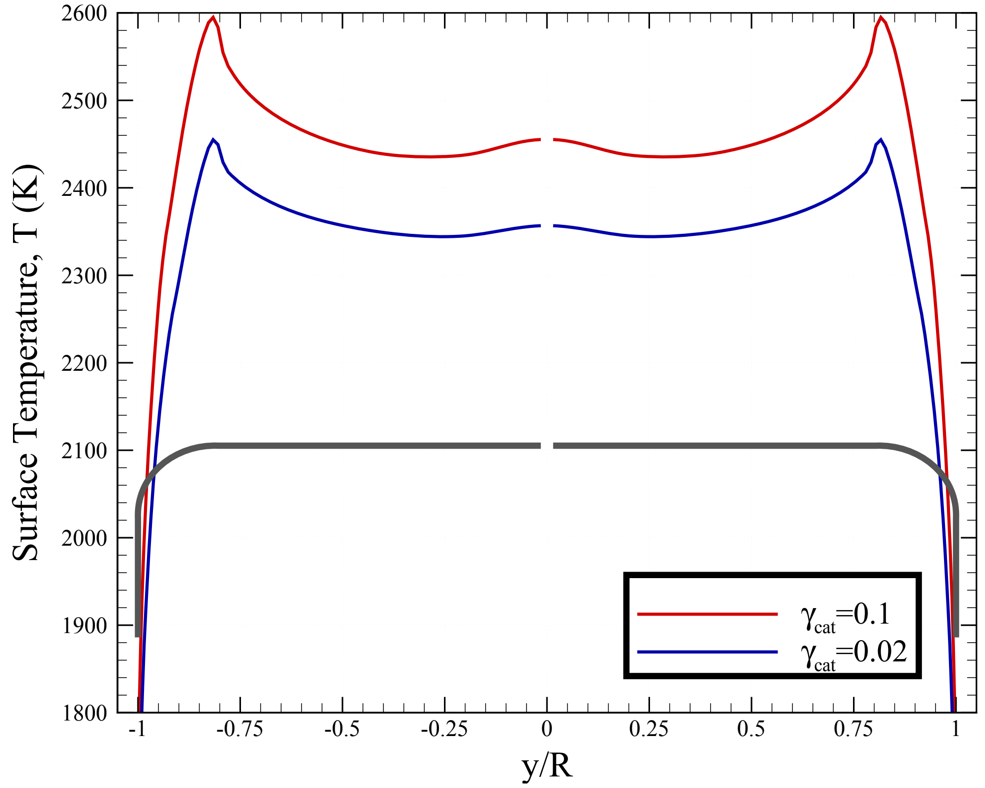

Full Disclosure

Opportunities for Further Enhancement

1. **Linear Solver Strategy:** Preconditioned GMRES is highly effective but potentially overkill for early, highly nonlinear transients. Mixed implicit/explicit schemes may provide a fast alternative.
2. **Improved Shock Capturing:** Robust shock capturing is still a challenge. Current scheme is fragile on bad meshes, and often convergence stalls.

Additional Focus Areas

1. Physics Modeling
   - Weakly Ionized Flows
   - Additional turbulence models
   - Fully coupled radiative transport
2. Unsteady ablation coupling
3. Adjoints
   - Sensitivity analysis
   - Adaptivity

Thank you!

Questions?